

# **(2,2'-bipyridyl)Re(CO)<sub>3</sub>Cl functionalized poly (3-hexylthiophene) as Third Generation Conducting Polymer for its Potential Application toward Electro- and Photochemical CO<sub>2</sub> Reduction**

## **BACHELOR THESIS**

to obtain the academic degree  
**Bachelor of Science**

in the Bachelor study program  
**TECHNICAL CHEMISTRY**

Submitted by  
**Gottfried Aufischer**

Carried out at  
**Linz Institute for Organic Solar Cells (LIOS) / Institute of Physical Chemistry**

Supervised by  
**Univ. Prof. Mag. Dr. DDr. h.c. Niyazi Serdar Sariciftci**

Guidance:  
**Dr. Elisa Tordin, Dr. Engelbert Portenkirchner**

**Wels, July 2014**

**Contents:**

<b>1. Introduction.....</b>	<b>2</b>
<b>2. <i>P3[Re]HT</i> Monomer Synthesis .....</b>	<b>4</b>
2.1. Synthesis of 3-(6-bromohexyl)thiophene.....	4
2.2. Synthesis of 4-methyl-4'-(7-(3-thienyl)-heptyl)-2,2'-bipyridine .....	6
2.3. Synthesis of <i>fac</i> -[Re(4-methyl-4'-(7-(3-thienyl)-heptyl)-2,2'-bipyridine)(CO) <sub>3</sub> Cl], <i>3[Re]HT</i> .....	8
<b>3. Electrochemical Polymerization &amp; Characterization .....</b>	<b>11</b>
3.1. Poly(thiophene).....	11
3.2. Poly(3-hexylthiophene) .....	14
3.3. Rhenium complex functionalized poly(thiophene), <i>P3[Re]HT</i> .....	16
<b>4. Cyclic voltammetry studies on electrochemical CO<sub>2</sub> reduction .....</b>	<b>23</b>
4.1. Poly(thiophene).....	23
4.2. Poly(3-hexylthiophene) .....	24
4.3. <i>P3[Re]HT</i> .....	25
<b>5. Summary and Outlook.....</b>	<b>28</b>

## 1. Introduction

In order to serve the current energy supply of our civilization, large amounts of fossil fuels are burnt. But with that several problems appear. During the combustion of these fuels, CO<sub>2</sub> is released which is considered to be a main greenhouse gas. Together with the fact that fossil fuel resources are limited, Carbon Capture and Utilization (CCU) has awoken scientific interest.<sup>[1-3]</sup> Especially the production of synthetic carbon based fuels using atmospheric carbon dioxide and renewable energy sources is a promising approach to tackle these problems.<sup>[4-6]</sup>

Since carbon dioxide is a very stable molecule, the use of suitable catalyst materials is essential for the reduction of CO<sub>2</sub> to CO. In terms of reasonable activities and lifetimes, metal complex compounds with bipyridine ligands exhibit proper traits.<sup>[7-9]</sup> Particularly the complex *fac*-[Re(2,2'-bipyridyl)(CO)<sub>3</sub>Cl] first prepared by Ziesel and Lehn et al. in 1984, shows high Faradaic efficiencies and stable performance over several hours of CO<sub>2</sub> electrolysis.<sup>[10,11]</sup>

Although homogenous catalysis is easier to characterize and mechanistically better understood than heterogeneous catalysis, it has several disadvantages. For efficient CO<sub>2</sub> reduction large quantities of catalyst material are required, which is very expensive. Additionally, due to limited solubility properties of the catalyst only a small selection of different organic solvents is available that often do not feature proper CO<sub>2</sub> solubility. Moreover homogeneous catalysts sometimes undergo solution deactivation pathways. In organic solvents for example, dimer formation occurs while using Rhenium complexes with bipyridene ligands.<sup>[12]</sup> In order to overcome these problems one possibility is to go from homogeneous to heterogeneous catalysis by immobilizing the catalyst onto the electrode.

Common ways for the immobilization of redox catalysts onto solid electrodes are the integration of the active species in a polymer matrix<sup>[13-15]</sup> or the chemical modification of the ligand-molecule with a functional group allowing polymerization with the formation of a redox polymer.<sup>[16-18]</sup> In 1992 Sariciftci et al. introduced the idea of "third generation of conducting polymers" or functionalized conductive polymers, that are the result of coupling an active group (with a specific function) to the backbone of a conducting polymer.<sup>[19]</sup>

Because of their versatile properties and potential applications, in the last decades electrically conducting and semiconducting polymers have attracted a great deal of interest.<sup>[20]</sup> In this field, particular attention has been given to poly(thiophene) (*PT*) for its moisture and air stability.<sup>[21-23]</sup>

Therefore, the aim of this work is to functionalize poly(3-hexylthiophene) (*P3HT*) with *fac*-[Re(2,2'-bipyridyl)(CO)<sub>3</sub>Cl] for its potential application concerning electro- and photochemical CO<sub>2</sub> reduction.

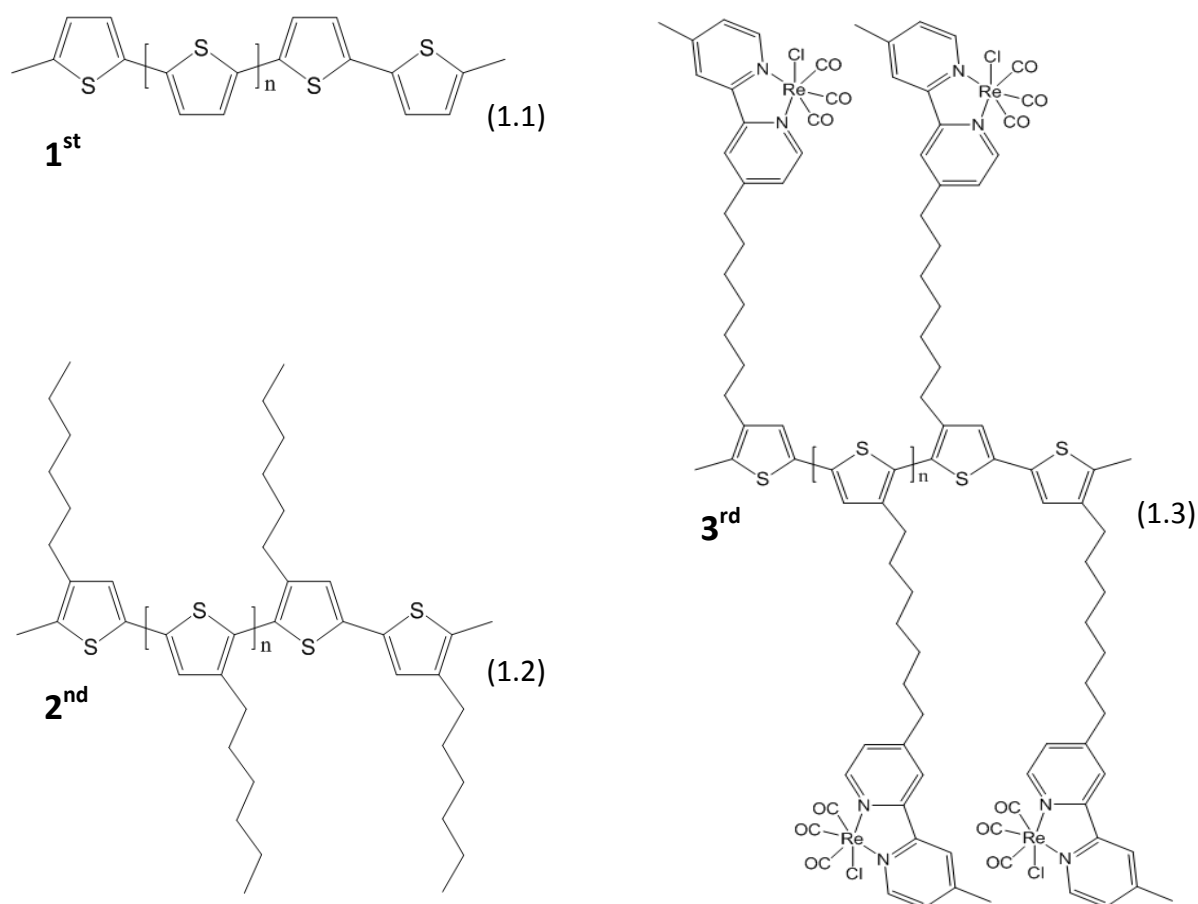


**Fig.1.** Schematic representation of three different conducting polymers investigated in this study, poly(thiophene) (1.1), poly(3-hexylthiophene) (1.2) and  $P3[Re]HT$  (1.3). Each of these polymers represents a different generation of conducting polymers.

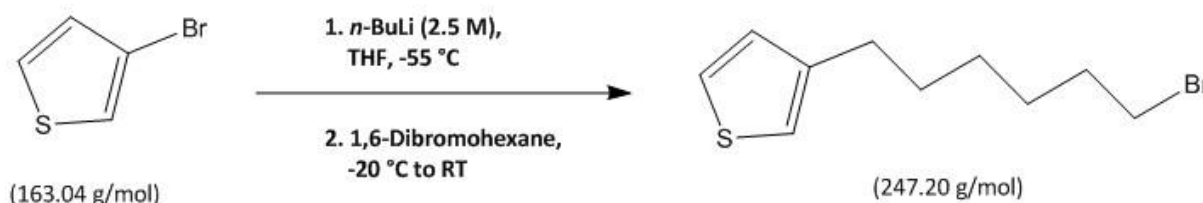
Figure 1 shows the schematic representation of three different conducting polymers investigated in this study, namely poly(thiophene) (1.1), poly(3-hexylthiophene) (1.2) and the polymer of *fac*-[Re(4-methyl-4'-(7-(3-thienyl)-heptyl)-2,2'-bipyridine)(CO)<sub>3</sub>Cl],  $P3[Re]HT$  (1.3). Each of these conjugated polymers represents a different generation of conducting polymers. Poly(thiophene) (1.1) exhibits good conductivity, but the material lacks reasonable solubility and processability. The introduction of aliphatic chains on the conducting polymer backbone structure leads to second generation of conductive polymers. In particular,  $P3HT$  (1.2) is a polythiophene bearing an *n*-hexyl chain on each thiophene unit. It maintains the interesting physical and chemical properties of the poly(thiophene) but it is characterized by high solubility and processability due to the aliphatic chains. The novel *fac*-[Re(2,2'-bipyridyl)(CO)<sub>3</sub>Cl] - functionalized  $P3HT$  (1.3) is a conjugated polymer with new physical and chemical properties for the potential applications of electro- and photochemical CO<sub>2</sub> reduction.

## 2. P3[Re]HT Monomer Synthesis

The general methodology was to synthesis a monomeric species that can be subsequently electropolymerized in order to obtain the novel P3[Re]HT.

### 2.1. Synthesis of 3-(6-bromohexyl)thiophene

#### 2.1.1. Reaction scheme



**Scheme 1.** Schematic representation of the reaction of 3-bromothiophene to 3-(6-bromohexyl)thiophene.<sup>[24]</sup>

#### 2.1.2. Procedure

This precursor was prepared by slight modifications of the reported methods.<sup>[24]</sup> 24.38 g (150 mmol) of 3-bromothiophene were dissolved in 180 mL of distilled *n*-hexane and cooled down to -55 °C. The cooling bath was prepared in a Dewar vessel by adding liquid nitrogen to acetone. 63 mL (158 mmol) of 2.5 M *n*-butyllithium in *n*-heptane were added drop wise and the resulting solution was stirred for 10 minutes. Anhydrous THF was added dropwise till the white lithium-thiophene salt precipitate (about 21 mL). The mixture was stirred for 1 h at -55 °C. The emulsion was then allowed to warm up slowly to -20 °C. After that, 90 mL (590 mmol) of 1,6-dibromohexane were added to the reaction mixture which was subsequently allowed to warm up to room temperature. After 3 h of stirring the emulsion was quenched with water and extracted with Et<sub>2</sub>O (3 x 100 mL). After drying with sodium sulfate, the solvent of the combined organic phases was removed *via* rotary evaporator. The excess of unreacted 1,6-dibromohexane was distilled out under vacuum and the residue was purified by column chromatography on silica as stationary phase and chloroform/*n*-hexane (1:1) as eluent. 10.11 g (41 mmol) of 3-(6-bromohexyl)thiophene as colorless oil were obtained with a yield of 27 %.

#### 2.1.3. Analysis of the product

<sup>1</sup>H-NMR (300 MHz, CDCl<sub>3</sub>):  $\sigma$ /ppm = 7.26 - 7.22 (m, 1H, thienyl), 6.94 - 6.92 (m, 2H, thienyl), 3.43 - 3.38 (t, 2H, hexyl), 2.66 - 2.59 (t, 2H, hexyl), 1.91 - 1.81 (m, 2H, hexyl), 1.69 - 1.59 (m, 2H, hexyl), 1.54 - 1.30 (m, 4H, hexyl).

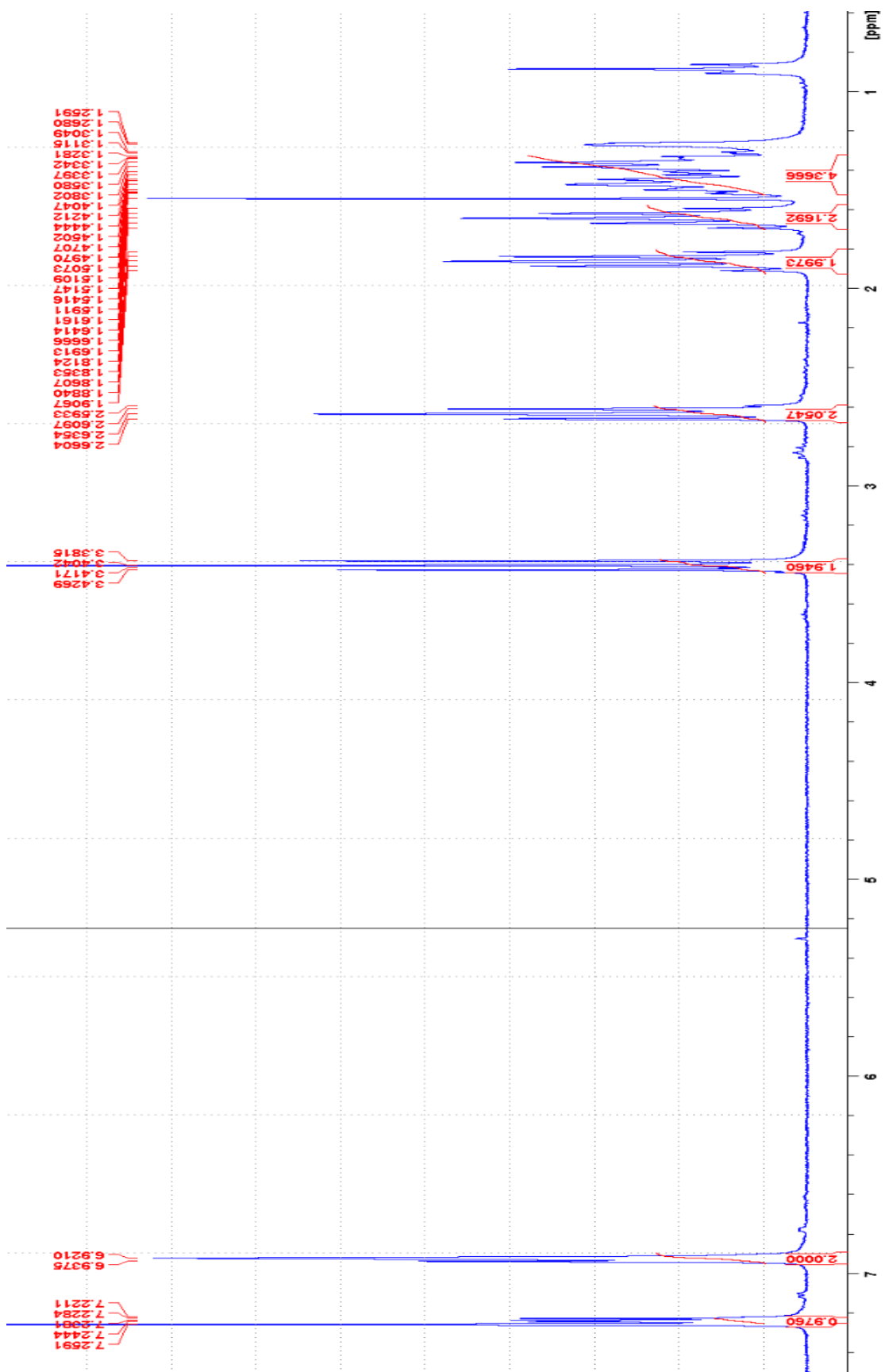
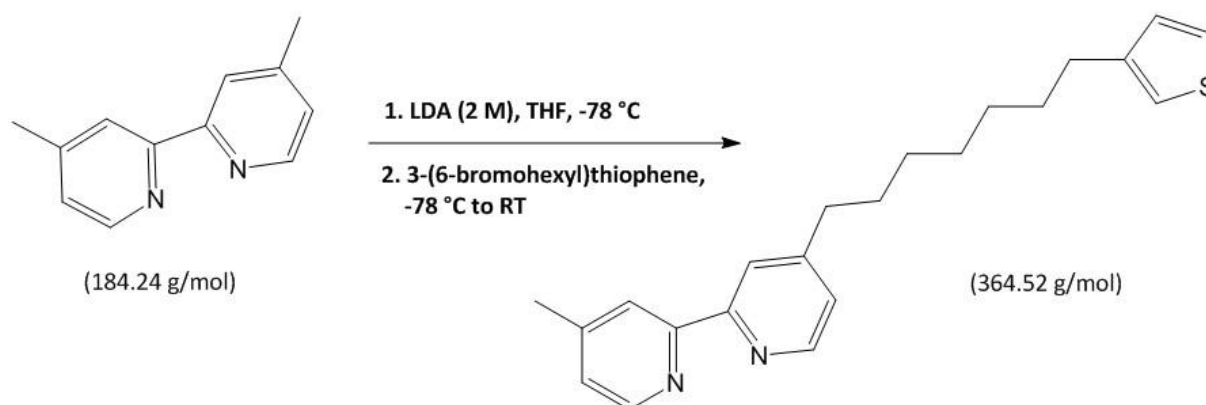


Fig.2.  $^1\text{H-NMR}$  of 3-(6-bromohexyl)-thiophene in  $\text{CDCl}_3$ .

## 2.2. Synthesis of 4-methyl-4'-(7-(3-thienyl)-heptyl)-2,2'-bipyridine

### 2.2.1. Reaction scheme



**Scheme 2.** Schematic representation of the reaction of 4,4'-dimethyl-2,2'-bipyridene and 3-(6-bromohexyl)thiophene to 4-methyl-4'-(7-(3-thienyl)-heptyl)-2,2'-bipyridine.<sup>[25]</sup>

### 2.2.2. Procedure

This compound was prepared by slight modifications of the reported methods.<sup>[25]</sup> 746 mg (4.05 mmol) of 4,4'-dimethyl-2,2'-bipyridene were dissolved in 40 mL of anhydrous THF and cooled down to -80 °C. The cooling bath was prepared in a Dewar vessel by adding liquid nitrogen to acetone. 2.05 mL (4.1 mmol) of 2 M lithium-diisopropylamide in THF/*n*-heptane was dissolved in 5 mL anhydrous THF, cooled down to -80 °C and slowly added to the reaction mixture. Within a few minutes it turned deep brownish black. After 30 min a solution of 1.006 g (4.07 mmol) of 3-(6-bromo-hexylthiophene) in 5 mL of anhydrous THF was added to the mixture at -80 °C. The solution was warmed up and within 2 h it reached -20 °C. At that point the cooling bath was removed. When the reaction mixture reached room temperature, it was quenched with water then extracted with Et<sub>2</sub>O (3 x 50 mL). The combined organic phases were dried with sodium sulfate, and the solvent was removed via rotary evaporator. After column chromatography on neutral alumina and *n*-hexane/chloroform (1:1) as eluent, 184 mg (0.67 mmol) of 50 % pure white product were isolated (yield of 8 %). The remain 50 % consist of unreacted 4,4'-dimethyl-2,2'-bipyridene.

### 2.2.3. Analysis of the product

<sup>1</sup>H-NMR (300 MHz, CDCl<sub>3</sub>):  $\sigma$ /ppm = 8.56 - 8.52 (m, 2H, bipyridyl), 8.23 (s, 2H, bipyridyl), 7.23 - 7.21 (m, 1H, thienyl), 7.13 - 7.10 (m, 2H, bipyridyl), 6.92 - 6.90 (m, 2H, thienyl), 2.70 - 2.58 (m, 4H, heptyl), 2.43 (s, 3H, CH<sub>3</sub>-), 1.70 - 1.58 (m, 4H, heptyl), 1.35 (s, 6H, heptyl).

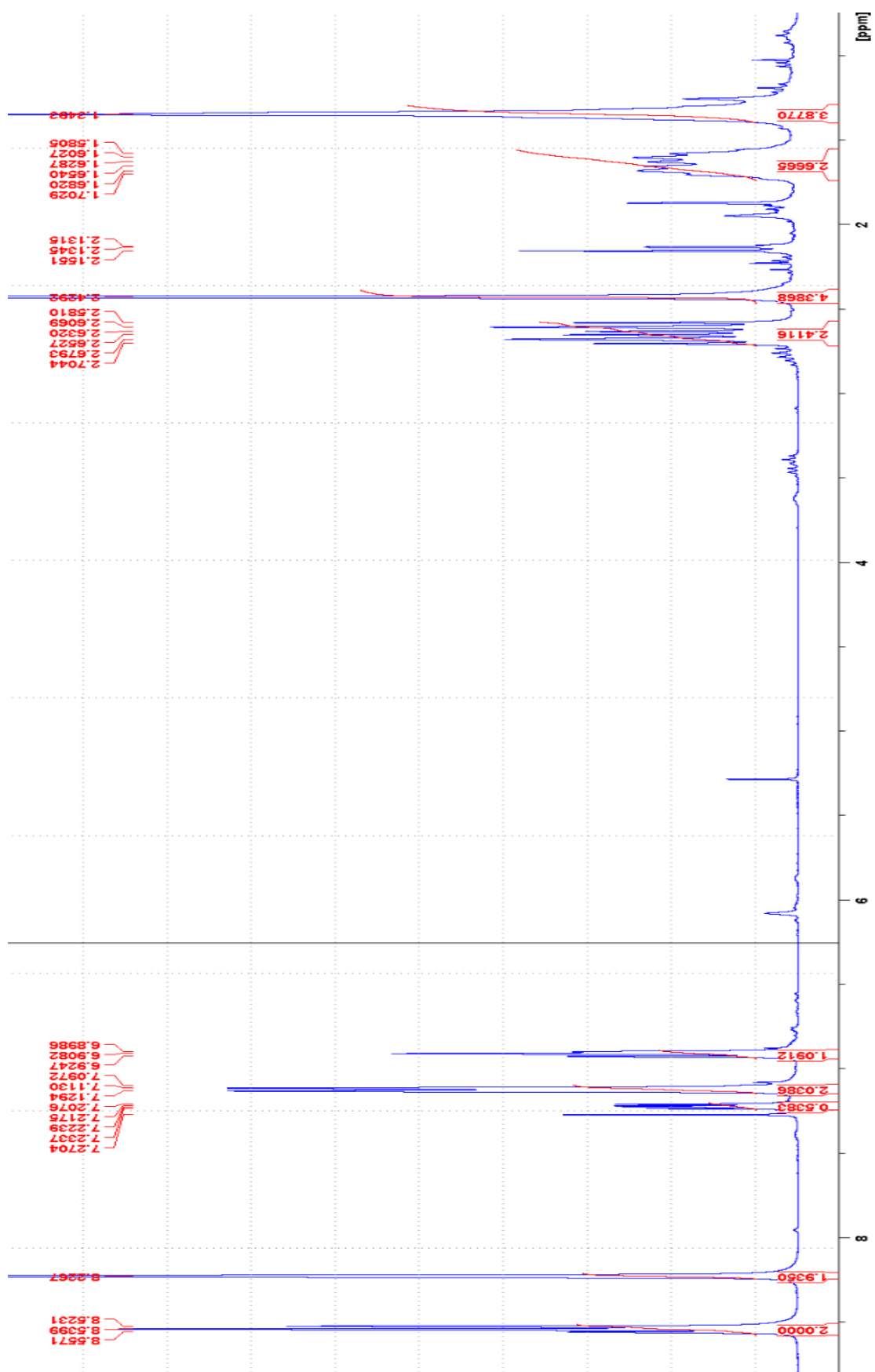
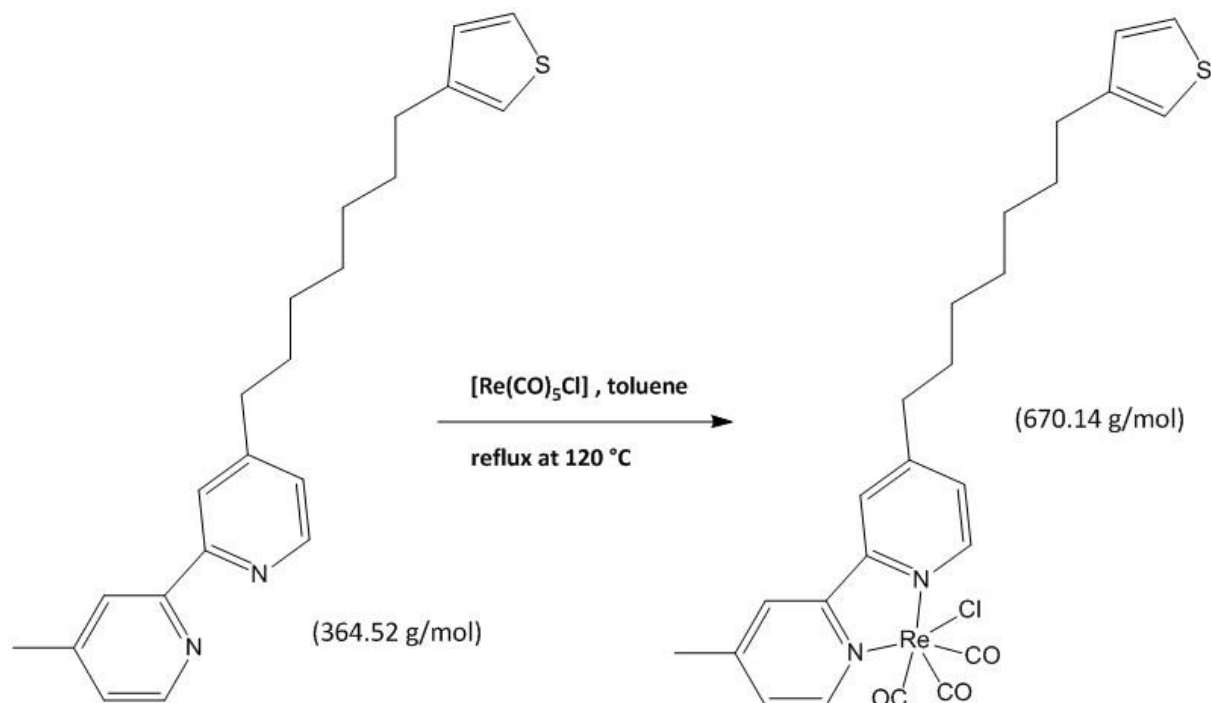


Fig.3. <sup>1</sup>H-NMR of 4-methyl-4'-(7-(3-thienyl)-heptyl)-2,2'-bipyridine in CDCl<sub>3</sub>.

## 2.3. Synthesis of *fac*-[Re(4-methyl-4'-(7-(3-thienyl)-heptyl)-2,2'-bipyridine)(CO)<sub>3</sub>Cl], 3[Re]HT

### 2.3.1. Reaction scheme



**Scheme 3.** Schematic representation of the complexation of 4-methyl-4'-(7-(3-thienyl)-heptyl)-2,2'-bipyridine to *fac*-[Re(4-methyl-4'-(7-(3-thienyl)-heptyl)-2,2'-bipyridine)(CO)<sub>3</sub>Cl].

### 2.3.2. Procedure

251 mg (0.693 mmol) of [Re(CO)<sub>5</sub>Cl] were dissolved under stirring in 40 mL of toluene at a temperature of 60 °C. 184 mg (0.671 mmol) of 50 % pure 4-methyl-4'-(7-(3-thienyl)-heptyl)-2,2'-bipyridine were added to the hot solution and refluxed for 1 hour. Within the first ten minutes the solution turned yellow and finally orange. The solvent was then removed on the rotary evaporator and the mixture of products was separated via column chromatography on neutral alumina and toluene/ethylacetate (4:1) as the eluent. 174 mg (0.26 mmol) of the yellow product *fac*-[Re(4-methyl-4'-(7-(3-thienyl)-heptyl)-2,2'-bipyridine)(CO)<sub>3</sub>Cl] were isolated with an yield of 77 %.



(4.1)



(4.2)

**Fig.4.** Photo of the reaction apparatus (4.1) and the final, dry product (4.2).

---

### 2.3.3. Analysis of the product

$^1\text{H-NMR}$  (300 MHz,  $\text{CDCl}_3$ ):  $\sigma/\text{ppm}$  = 8.89 - 8.86 (t, 2H, bipyridyl), 7.98 - 7.95 (d, 2H, bipyridyl), 7.33 - 7.30 (m, 2H, bipyridyl), 7.26 - 7.23 (m, 1H, thienyl), 6.94 - 6.92 (m, 2H, thienyl), 2.80 - 2.74 (t, 2H, heptyl), 2.66 - 2.61 (t, 2H, heptyl), 2.56 (s, 3H,  $\text{CH}_3$ -), 1.70 - 1.61 (m, 4H, heptyl), 1.38 (s, 6H, heptyl).

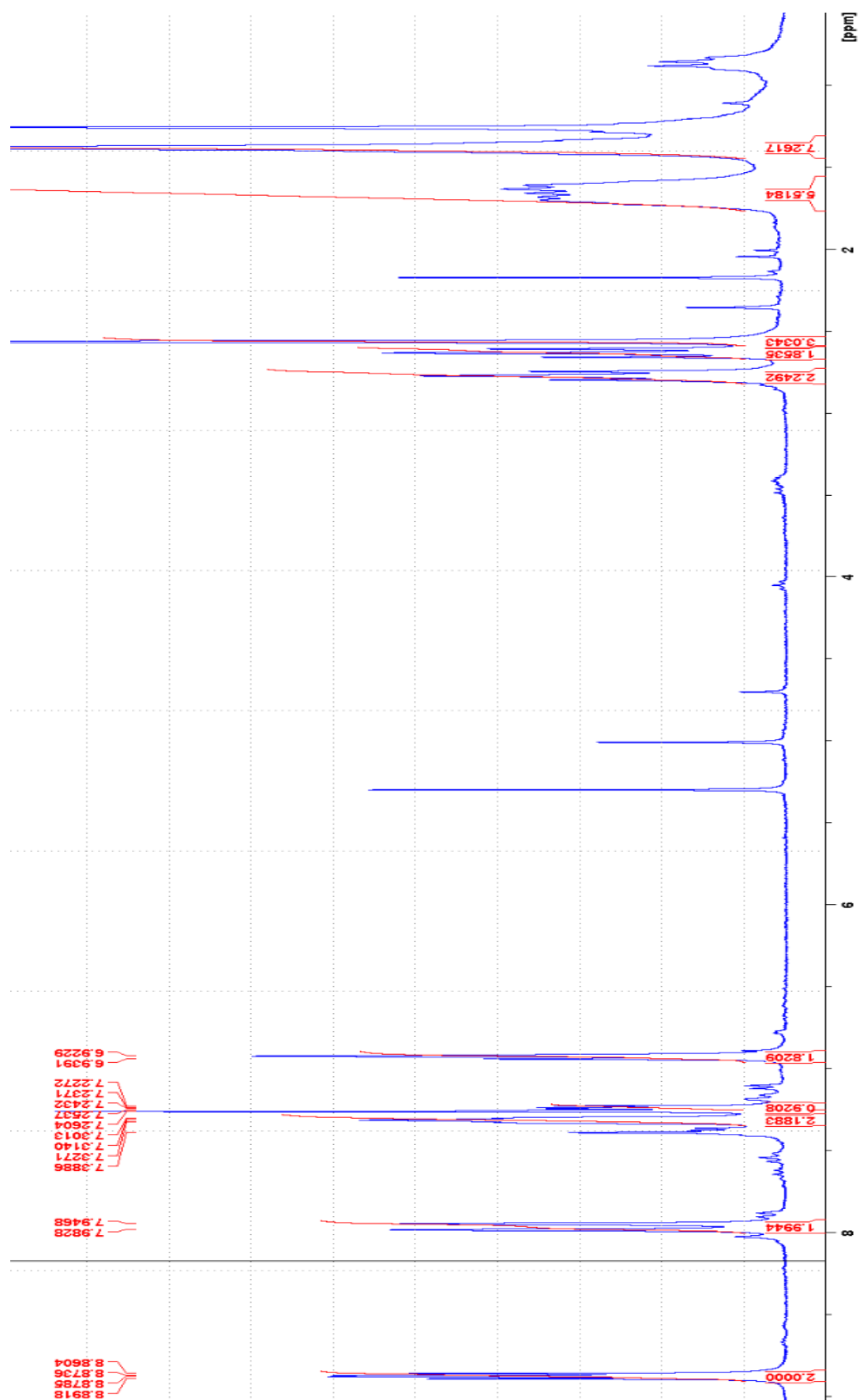
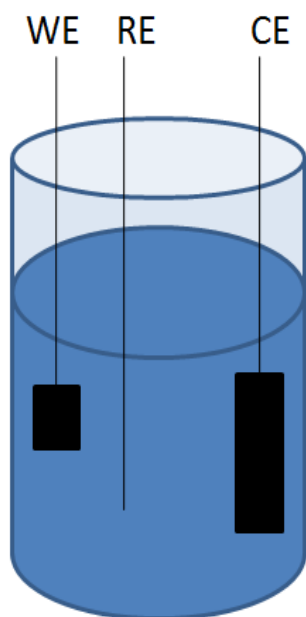


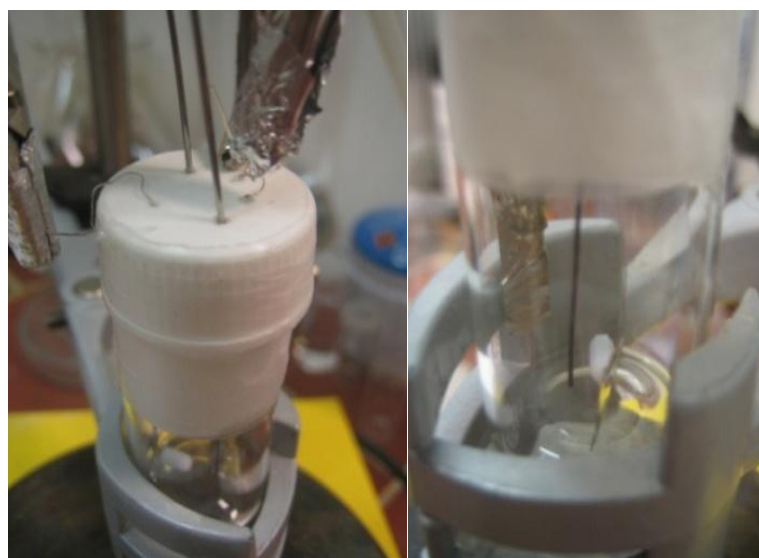
**Fig.5.**  $^1\text{H-NMR}$  of  $\text{fac-}[\text{Re}(\text{4-methyl-4'-(7-(3-thienyl)-heptyl)-2,2'-bipyridine})(\text{CO})_3\text{Cl}]$  in  $\text{CDCl}_3$ .

### 3. Electrochemical Polymerization & Characterization

Cyclic voltammetric measurements including electrochemical polymerizations and characterizations were carried out inside a one-compartment cell using a platinum sheet working electrode (WE), a platinum sheet counter electrode (CE) and a Ag/AgCl quasi reference electrode (RE) calibrated with ferrocene. The electrolyte solutions were purged with nitrogen under stirring for 15 minutes before cyclic voltammograms were recorded.



(6.1)



(6.2)

**Fig.6.** Schematic (6.1) and applied (6.2) cell set-up for cyclic voltammetric measurements. A platinum sheet was used for working electrode (WE) and counter electrode (CE) respectively. As quasi reference electrode (RE) a silver wire covered with silver chloride was used.

#### 3.1. Poly(thiophene)

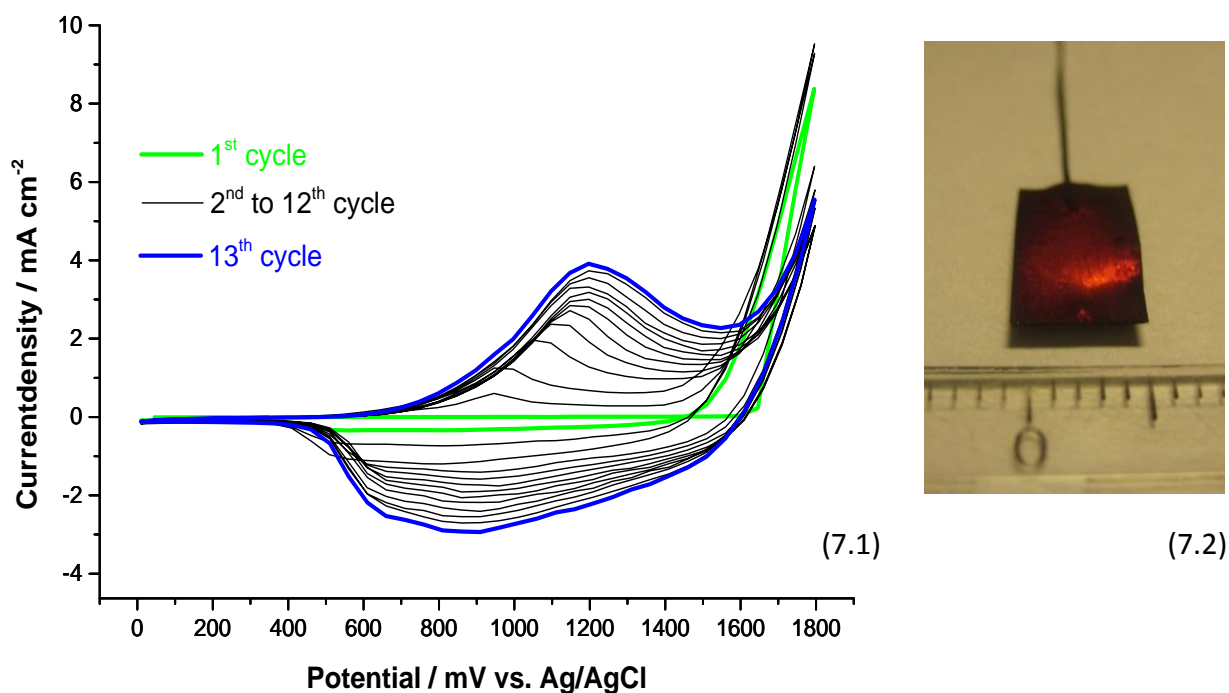
Electroactive monomers including thiophenes can be polymerized to form conducting and semiconducting polymers. Such polymers can be produced chemically or electrochemically<sup>[26]</sup>. The electropolymerization has several advantages for the deposition of organic conducting or semiconducting films onto conducting materials. By adjusting the electrochemical parameters of an electropolymerization process, the rate of polymer nucleation and therefore the growth of the film can be controlled. Also the film thickness can be modified by regulating the amount of charge that passes during the process of deposition. Furthermore the film morphology can be controlled to a certain extent by choosing proper solvents and supporting electrolytes.<sup>[27]</sup> In this work, electropolymerizations were performed potentiodynamically which was shown to result in the formation of conducting polymer matrixes forming disordered spatial chains.<sup>[28]</sup>

### 3.1.1. Electropolymerization of thiophene to poly(thiophene)

Reaction scheme:



**Scheme 4.** Schematic representation of the electropolymerization of thiophene to poly(thiophene).



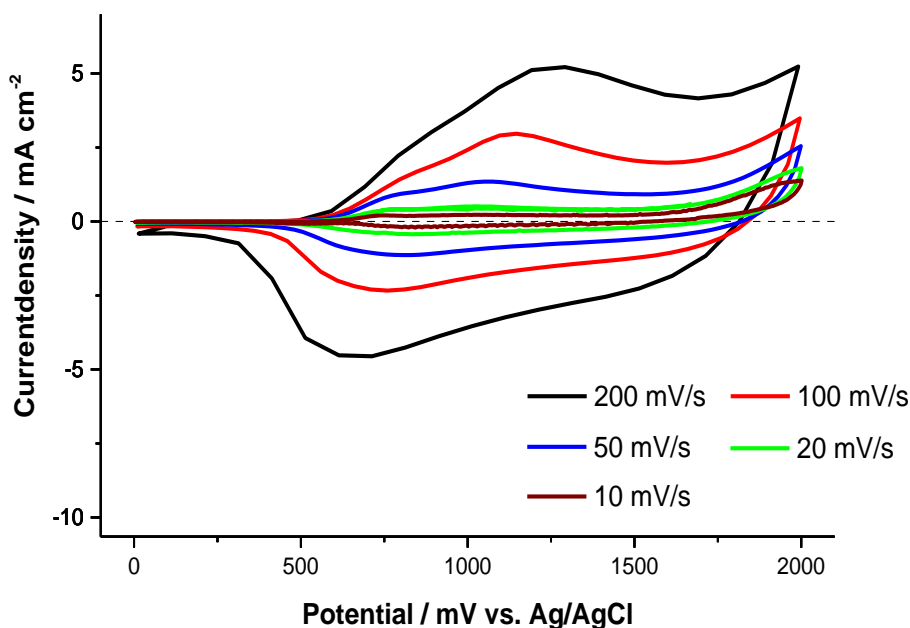
**Fig.7.** Cyclic voltammograms of the potentiodynamic electropolymerization of 0.1 M thiophene to poly(thiophene) (7.1) in ACN solution containing 0.1 M TBAPF<sub>6</sub> as supporting electrolyte. First scan (green line) and last scan (blue line). The cyclic voltammograms were recorded at a scan rate of 100 mV s<sup>-1</sup> inside the glove box using a Pt working electrode (WE), a Pt counter electrode (CE) and a Ag/AgCl quasi reference electrode (RE). Picture of the electropolymerized poly(thiophene) on the platinum sheet working electrode (7.2).

Fig. 7 shows the potentiodynamic electropolymerization of 0.1 M thiophene to poly(thiophene) (7.1) in ACN solution containing 0.1 M TBAPF<sub>6</sub> as supporting electrolyte. The successive film formation is indicated by an increase in the current density of each cycle. The first scan is depicted in green and the last scan in blue respectively. After the electropolymerization the Pt working electrode was fully covered with a continuous crimson red film, as can be seen in the picture in Fig.7 (7.2). The mechanism for the polymerization has been reported to proceed via a radical coupling mechanism resulting in  $\alpha$ - $\alpha$  linkages.<sup>[29]</sup> Following the progress of the polymerization, one can observe a shift to lower oxidation potentials upon increasing scan numbers. This trend can be understood by the fact that the

$\alpha$ - $\alpha$  linkage are a combination of monomer and oligomer radicals where the polymerization reaction occurs at lower potentials on existing polymer than on a bare metal surface.<sup>[30]</sup> Repeated cycling resulted in a potential shift of the wave current maximum.

This can be related to the fact that during film growth, the electrical resistance in the polymer film and the overpotential needed to overcome the resistance increases.<sup>[31]</sup> The cyclic voltammograms were recorded at a scan rate of  $100 \text{ mV s}^{-1}$  inside the glove box using a platinum sheet working and counter electrode and a Ag/AgCl quasi reference electrode.

### 3.1.2. Characterization of poly(thiophene)



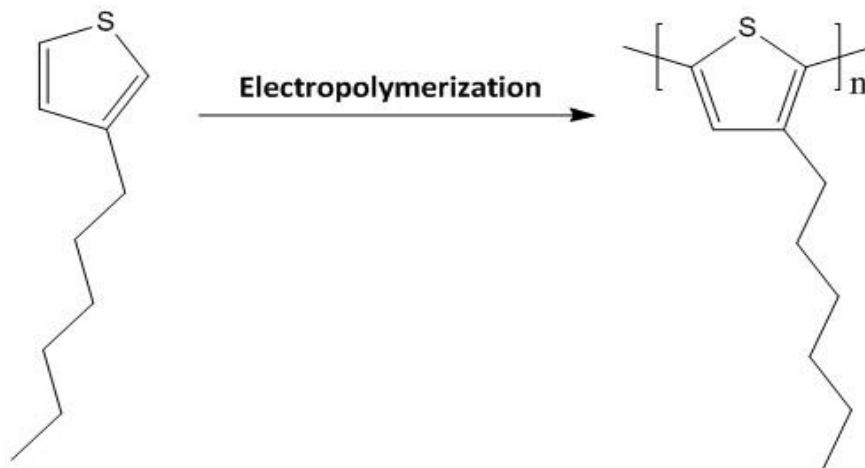
**Fig.8.** Cyclic voltammograms of poly(thiophene) electrochemically polymerized on platinum plate electrode in ACN solution containing 0.1 M TBAPF<sub>6</sub> at different scan rates from 200 (black line) to 10 (brown line)  $\text{mV s}^{-1}$ . The ferrocene peak half-wave potential  $E_{1/2 \text{Fc}/\text{Fc}^+}$  was measured at 415 mV vs. Ag/AgCl.

Fig.8 shows the electroactivity of the poly(thiophene) electrochemically polymerized film on a platinum plate electrode at various scan rates from  $200 \text{ mV s}^{-1}$  (black line) to  $10 \text{ mV s}^{-1}$  (brown line). As can be seen, the intensity of the redox wave currents is proportional to the scan rate and the polymer film exhibits reversible redox behavior. A plot of peak current vs. scan rate reveals a linear dependence suggesting that the redox process is not any more diffusion controlled as predicted by the Randles-Sevcik equation.<sup>[32]</sup> This further confirms the formation of an electroactive film immobilized on the Pt electrode surface.<sup>[33]</sup>

## 3.2. Poly(3-hexylthiophene)

### 3.2.1. Electropolymerization of 3-hexylthiophene to poly(3-hexylthiophene)

Reaction scheme:



**Scheme 5.** Schematic representation of the electropolymerization of 3-hexylthiophene to poly(3-hexylthiophene).

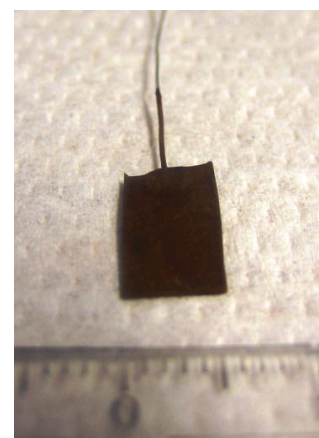
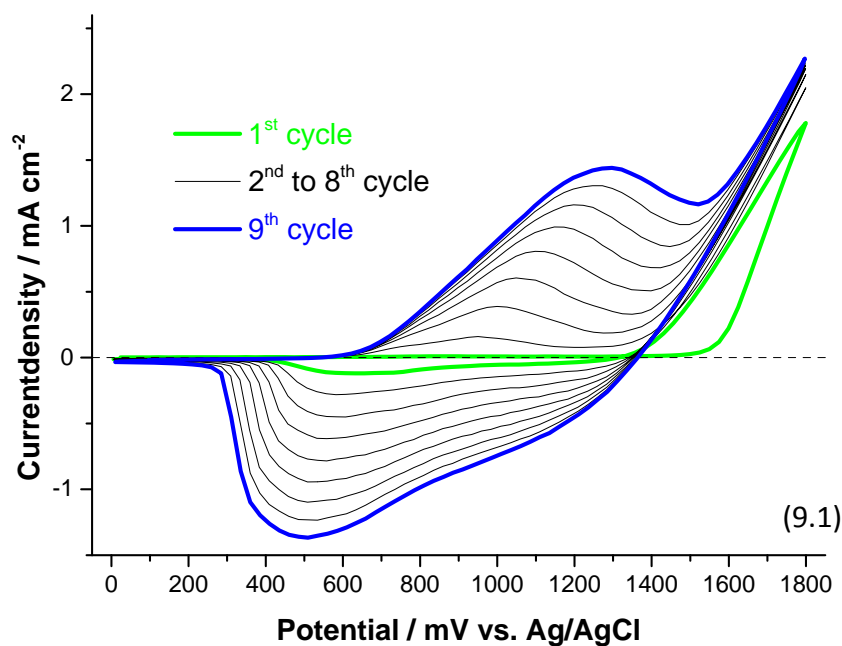


**Fig.9.** Cyclic voltammograms of the potentiodynamic electropolymerization of 0.056 M 3-hexylthiophene to poly(3-hexylthiophene) (9.1) in propylene carbonate solution containing 0.1 M TBAPF<sub>6</sub> as supporting electrolyte. First scan (green line) and last scan (blue line). The cyclic voltammograms were recorded at a scan rate of 50 mV s<sup>-1</sup> inside the glove box using a Pt working electrode (WE), a Pt counter electrode (CE) and a Ag/AgCl quasi reference electrode (RE). Picture of the electropolymerized poly (3-hexylthiophene) on the platinum sheet working electrode (9.2).

Fig.9 shows the potentiodynamic electropolymerization of 0.056 M 3-hexylthiophene to poly(3-hexylthiophene) (9.1) in propylene carbonate solution containing 0.1 M TBAPF<sub>6</sub> as supporting electrolyte. The successive film formation is indicated by an increase in the current density of each cycle. The first scan is depicted in green and the last scan in blue respectively. After electropolymerization the platinum sheet working electrode was fully covered with a continuous dark red film, as can be seen in the picture in Fig.9 (9.2). The mechanism for the polymerization has been reported to proceed via a radical coupling similar to the case of the poly(thiophene) described before. Also, following the progress of the polymerization, one can observe again a shift to lower oxidation potentials upon increasing scan numbers. The cyclic voltammograms were recorded at a scan rate of 50 mV s<sup>-1</sup> inside the glove box using a platinum sheet working and counter electrode and a Ag/AgCl quasi reference electrode.

### 3.2.2. Characterization of poly(3-hexylthiophene)

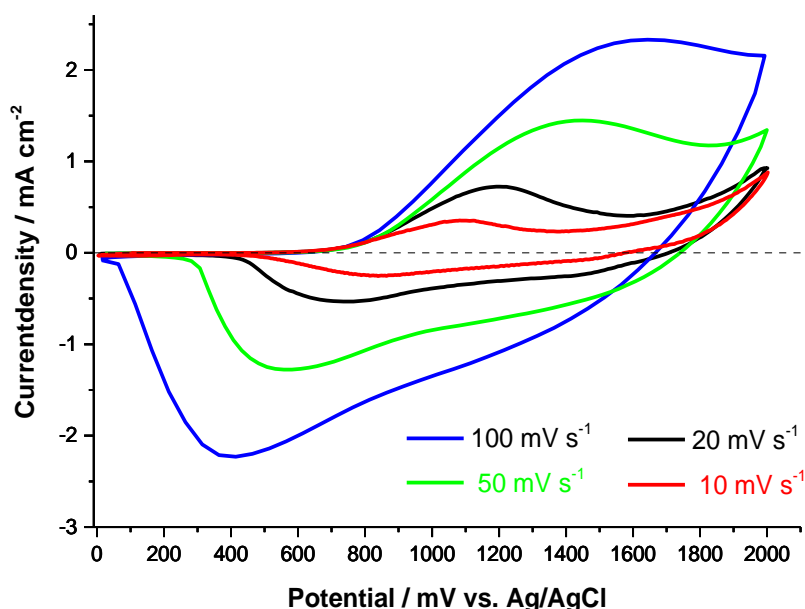


**Fig.10.** Cyclic voltammograms of poly(3-hexylthiophene) electrochemically polymerized on platinum plate electrode in propylene carbonate solution containing 0.1 M TBAPF<sub>6</sub> at different scan rates from 100 (blue line) to 10 (red line) mV s<sup>-1</sup>. The ferrocene peak half-wave potential  $E_{1/2 \text{Fc}/\text{Fc}^+}$  was measured at 428 mV vs. Ag/AgCl.

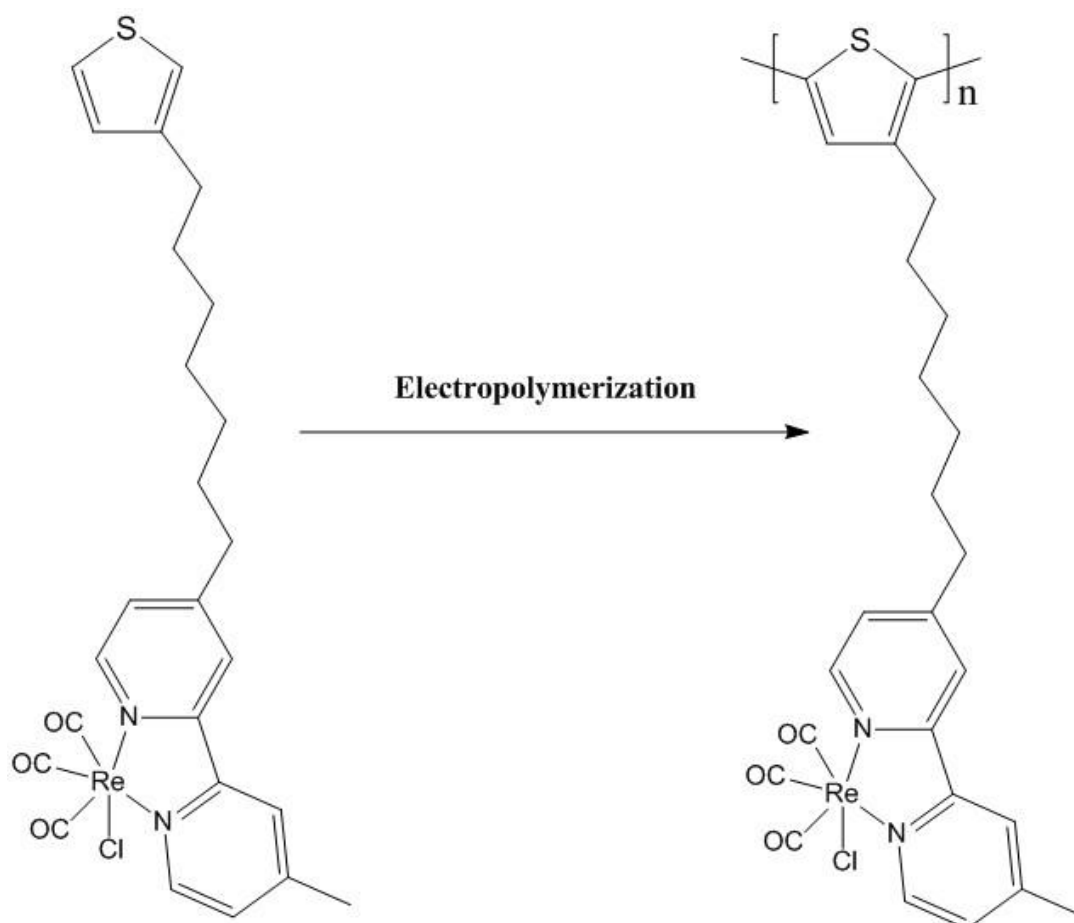
Fig.10 shows the electroactivity of the poly (3-hexylthiophene) electrochemically polymerized film on a platinum plate electrode at various scan rates from 100 mV s<sup>-1</sup> (blue line) to 10 mV s<sup>-1</sup> (red line). As can be seen, similar to the reported behavior of poly(thiophene) before (compare Fig.8), the intensity of the redox wave currents is proportional to the scan rate and the polymer film exhibits reversible redox behavior. Also in the study of poly(3-hexylthiophene) this fact further confirms the formation of an electroactive film immobilized on the platinum electrode surface.

Comparing the electrochemical characterization of poly(3-hexylthiophene) in Fig.10 to the poly(thiophene) in Fig.8, it can be stated that the conductivity of the film does not appear to be influenced significantly by the presence of the alkyl substituents on the 3-positions of the poly(thiophene) although one might expect a structural change in the film due to steric interactions which could result in lower conductivities. Generally it has been reported, that for poly(thiophene) as well as for poly(3-hexylthiophene) conductivities are in the order of  $1-100 \text{ S cm}^{-1}$  [29,34,35].

### 3.3. Rhenium complex functionalized poly(thiophene), *P3[Re]HT*

#### 3.3.1. Electropolymerization of *fac*-[Re(4-methyl-4'-(7-(3-thienyl)-heptyl)-2,2'-bipyridine)(CO)<sub>3</sub>Cl] to Rhenium complex functionalized poly(thiophene), *P3[Re]HT* "thin film"

Reaction scheme:



**Scheme 6.** Schematic representation of the electropolymerization of *fac*-[Re(4-methyl-4'-(7-thienylheptyl)-2,2'-bipyridine)(CO)<sub>3</sub>Cl] to *P3[Re]HT*.

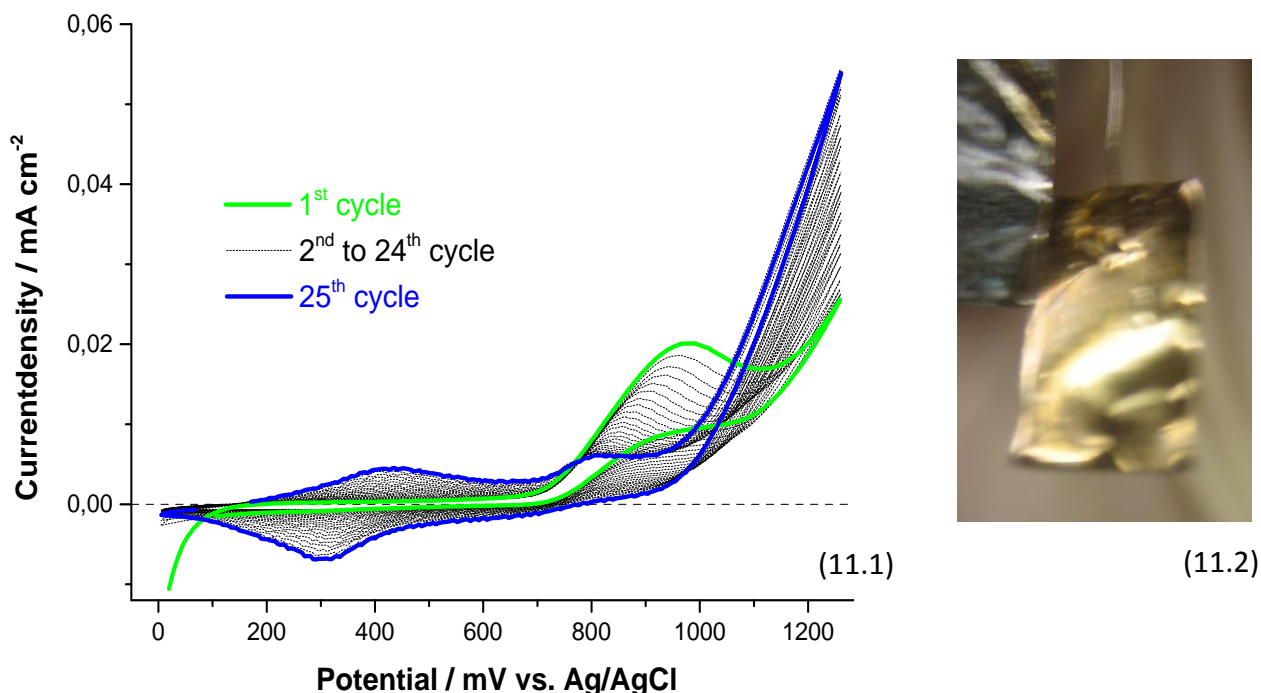


**Fig.11.** Cyclic voltammograms of the potentiodynamic electropolymerization of 15 mM *fac*-[Re(4-methyl-4'-(7-thienylheptyl)-2,2'-bipyridene(CO)<sub>3</sub>Cl)] to *P3[Re]HT* (11.1) in boron trifluoride ethyl etherate (BFEE). First scan (green line) and last scan (blue line). The cyclic voltammograms were recorded at a scan rate of 50 mV s<sup>-1</sup> outside the glove box using a Pt working electrode (WE), a Pt counter electrode (CE) and a Ag/AgCl quasi reference electrode (RE). Picture of the very thin *P3[Re]HT* film on the platinum sheet working electrode (11.2).

Fig.11 shows the potentiodynamic electropolymerization of 15 mM *fac*-[Re(4-methyl-4'-(7-thienylheptyl)-2,2'-bipyridene(CO)<sub>3</sub>Cl)] to *P3[Re]HT* in boron trifluoride ethyl etherate (BFEE). The successive film formation is indicated by an increase in the current density of each cycle. The first scan is depicted in green and the last scan in blue respectively. After electropolymerization the thin film on the platinum working electrode was barely visible.

Electropolymerization of *fac*-[Re(4-methyl-4'-(7-thienylheptyl)-2,2'-bipyridene(CO)<sub>3</sub>Cl)] to *P3[Re]HT* as the representative compound for the so called 3<sup>rd</sup> generation type of conducting polymer was difficult in the sense that the *fac*-[Re(2,2'-bipyridyl)(CO)<sub>3</sub>Cl] groups attached to the poly(thiophene) backbone undergo partly irreversible oxidation above a potential of 1300 mV vs. Ag/AgCl (compare Fig.12). One possible way to overcome this problem is to use boron trifluoride ethyl etherate (BFEE) which substantially lowers the required potential for electropolymerization.<sup>[36]</sup> Furthermore, the catalytic effect of BFEE enhances the growth of high-quality films of poly(thiophene) and its derivatives with good mechanical, electrical and thermal properties. BFEE has a relatively low conductivity and ranges from 3 x 10<sup>-4</sup> and 9 x 10<sup>-4</sup> S/cm. Due to the formation of [(C<sub>2</sub>H<sub>5</sub>)<sub>3</sub>O<sup>+</sup>][BF<sub>4</sub><sup>-</sup>] complex, BFEE becomes an electrolyte solution itself without addition of any salt necessary. Moreover, small amounts of water will form [H<sup>+</sup>][BF<sub>3</sub>OH<sup>-</sup>] species that act as electrolyte.<sup>[37]</sup>

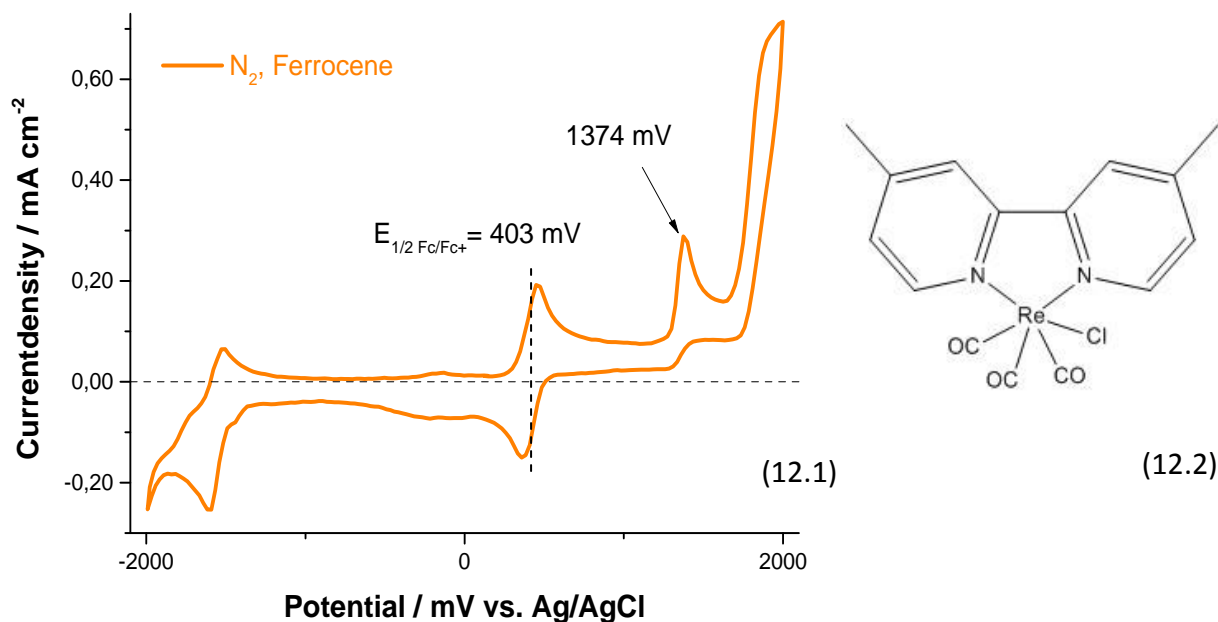


**Fig.12.** Cyclic voltammogram of 1 mM *fac*-[Re(4,4'-dimethyl-2,2'-bipyridyl)(CO)<sub>3</sub>Cl] in ACN solution containing 0.1 M TBAPF<sub>6</sub> as supporting electrolyte (12.1). The cyclic voltammogram was recorded at a scan rate of 50 mV s<sup>-1</sup> inside the glove box using a Pt working electrode (WE), a Pt counter electrode (CE) and a Ag/AgCl quasi reference electrode (RE). The ferrocene peak half-wave potential  $E_{1/2 \text{Fc/Fc}^+}$  was measured at 403 mV vs. Ag/AgCl. Schematic chemical structure of *fac*-[Re(4,4'-dimethyl-2,2'-bipyridyl)(CO)<sub>3</sub>Cl] (12.2).

Fig.12 shows the cyclic voltammogram of 1 mM *fac*-[Re(4,4'-dimethyl-2,2'-bipyridyl)(CO)<sub>3</sub>Cl] in ACN solution containing 0.1 M TBAPF<sub>6</sub> as supporting electrolyte. The cyclic voltammogram was recorded at a scan rate of 50 mV s<sup>-1</sup> inside the glove box using a platinum sheet working and counter electrode and a Ag/AgCl quasi reference electrode. A partly irreversible oxidation wave of *fac*-[Re(4,4'-dimethyl-2,2'-bipyridyl)(CO)<sub>3</sub>Cl] starts at around 1300 mV vs. Ag/AgCl.

Fig.13 shows the cyclic voltammogram of 1 mM 4,4'-dimethyl-2,2'-bipyridene in ACN solution containing 0.1 M TBAPF<sub>6</sub> as supporting electrolyte. The cyclic voltammogram was recorded at a scan rate of 50 mV s<sup>-1</sup> inside the glove box using a platinum sheet working and counter electrode and a Ag/AgCl quasi reference electrode.

Compared to the complexed ligand *fac*-[Re(4,4'-dimethyl-2,2'-bipyridyl)(CO)<sub>3</sub>Cl] (Fig.12), the free ligand 4,4'-dimethyl-2,2'-bipyridene (Fig.13) did not show a partly irreversible oxidation wave starting at around 1300 mV vs. Ag/AgCl.

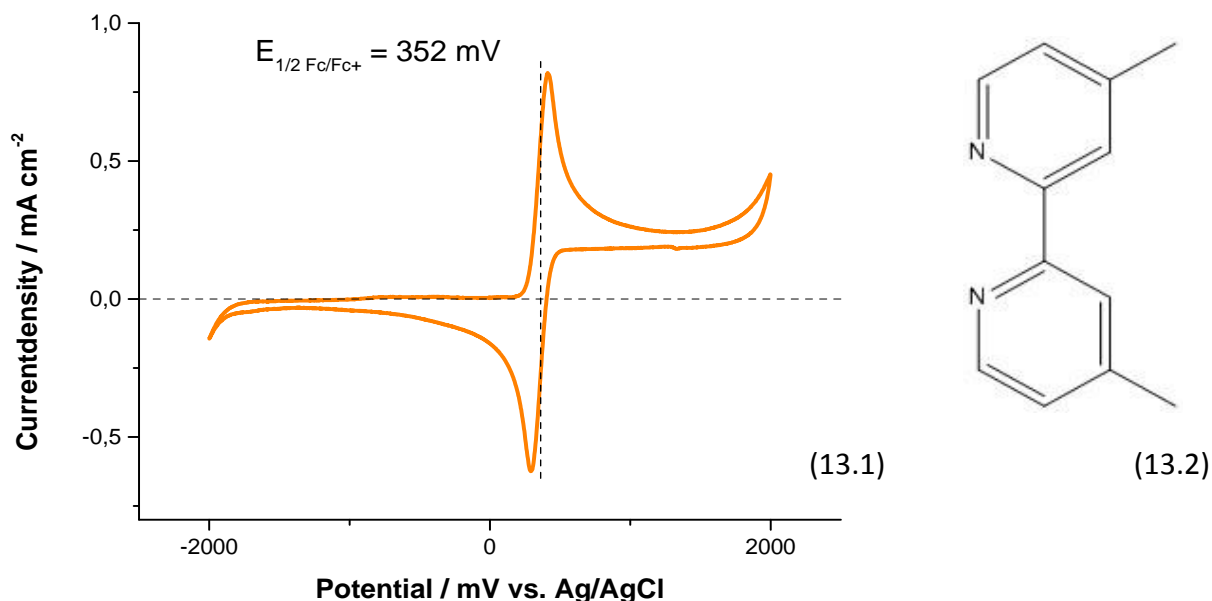


**Fig.13.** Cyclic voltammogram of 1 mM 4,4'-dimethyl-2,2'-bipyridene in ACN solution containing 0.1 M TBAPF<sub>6</sub> as supporting electrolyte (13.1). The cyclic voltammogram was recorded at a scan rate of 50 mV s<sup>-1</sup> inside the glove box using a Pt working electrode (WE), a Pt counter electrode (CE) and a Ag/AgCl quasi reference electrode (RE). The ferrocene peak half-wave potential  $E_{1/2 Fc/Fc^+}$  was measured at 352 mV vs. Ag/AgCl. Schematic chemical structure of 4,4'-dimethyl-2,2'-bipyridene (13.2).

### 3.3.2. Characterization of *P3[Re]HT*-"thin film"

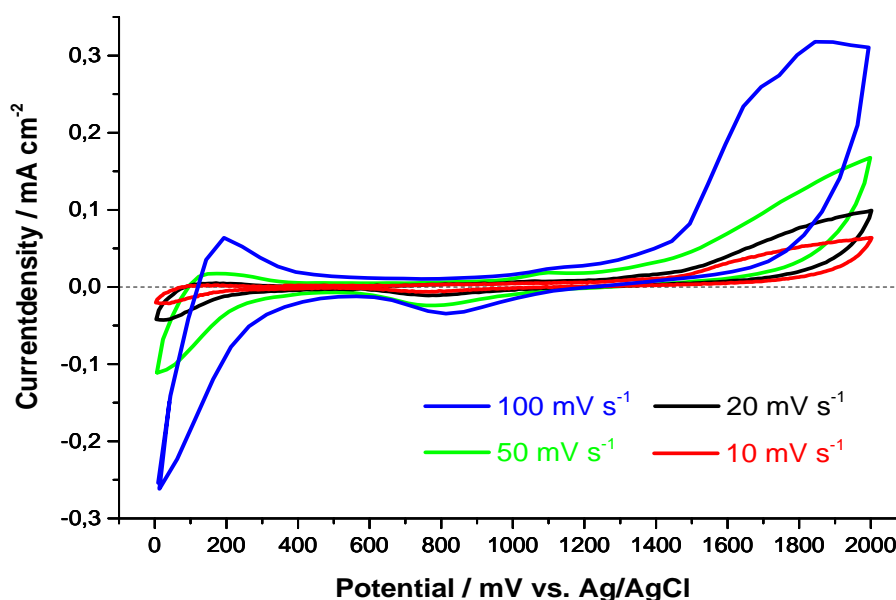


**Fig.14.** Cyclic voltammograms of a *P3[Re]HT*-"thin film" electrochemically polymerized on platinum plate electrode. The curves were recorded in propylene carbonate solution containing 0.1 M TBAPF<sub>6</sub> at different scan rates from 100 (blue line) to 10 (red line) mV s<sup>-1</sup>.

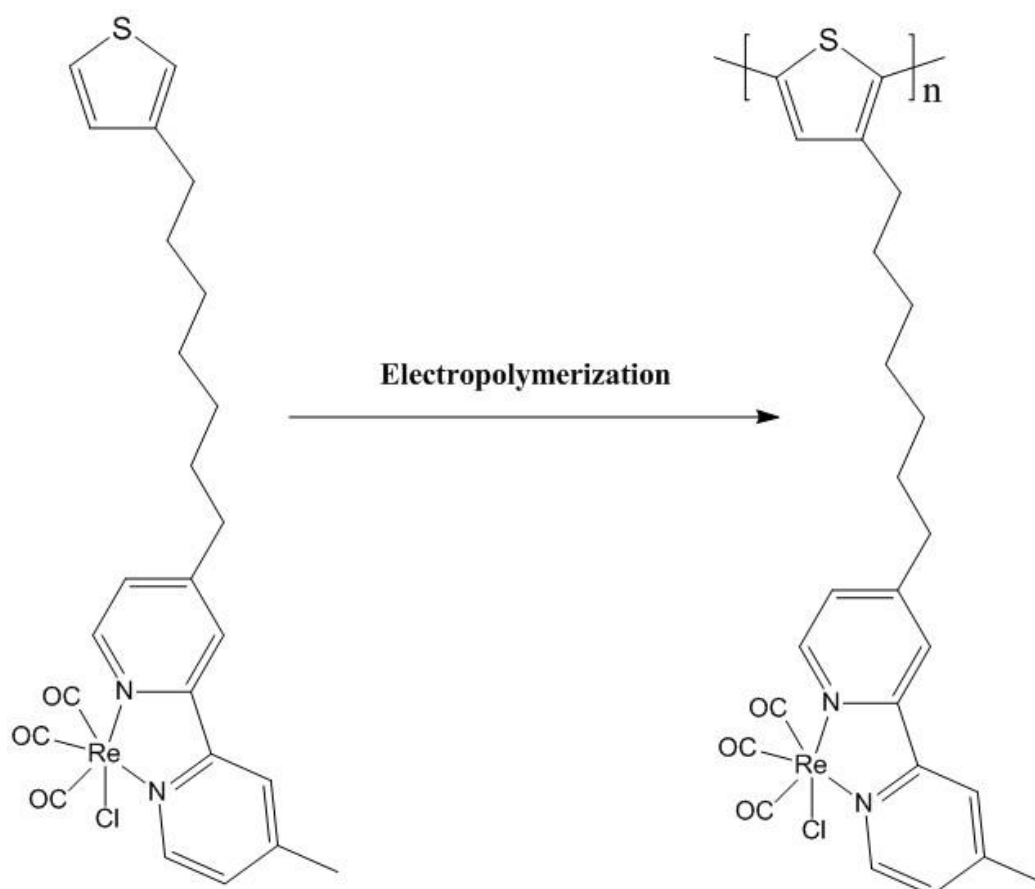
Fig.14 shows the electroactivity of *P3[Re]HT*-"thin film" in propylene carbonate solution containing 0.1 M TBAPF<sub>6</sub> at various scan rates from 100 mV s<sup>-1</sup> (blue line) to 10 mV s<sup>-1</sup> (red

line). As can be seen, similar to the reported behavior of poly(thiophene) and poly(3-hexylthiophene) before, the intensity of the redox wave currents is proportional to the scan rate and the polymer film exhibits reversible redox behavior. By comparing the electrochemical characterization of electropolymerized poly(3-hexylthiophene) (Fig.10) to *P3[Re]HT* presented here, it is obvious that the conductivity of the film decreases roughly by a factor of about 10 between the two electrodes studied.

The actual decrease in conductivity is expected to be even more prominent since the film of *P3[Re]HT* was substantially thinner than the poly(3-hexylthiophene). This might be due to the strong influence by the presence of the *fac*-[Re(2,2'-bipyridyl)(CO)<sub>3</sub>Cl] groups attached to the poly(thiophene) backbone. One might expect in this case a structural change in the film due to steric interactions which will result in conductivities substantially lower than 1-100 S cm<sup>-1</sup>.

### 3.3.3. Electropolymerization of *fac*-[Re(4-methyl-4'-(7-thienylheptyl)-2,2'-bipyridene)(CO)<sub>3</sub>Cl] to Rhenium complex functionalized poly(thiophene), *P3[Re]HT*-"thick film"

Reaction scheme:



**Scheme 7.** Schematic representation of the electropolymerization of *fac*-[Re(4-methyl-4'-(7-thienylheptyl)-2,2'-bipyridene)(CO)<sub>3</sub>Cl] to *P3[Re]HT*.

In order to prepare a thicker film of  $P3[Re]HT$ , the concentration of  $fac-[Re(4\text{-methyl-4'-(7\text{-thienylheptyl})-2,2'\text{-bipyridine}(\text{CO})_3\text{Cl})]$  in BFEE has to be increased. To overcome this problem a small amount of propylene carbonate (PPC) was added to BFEE.

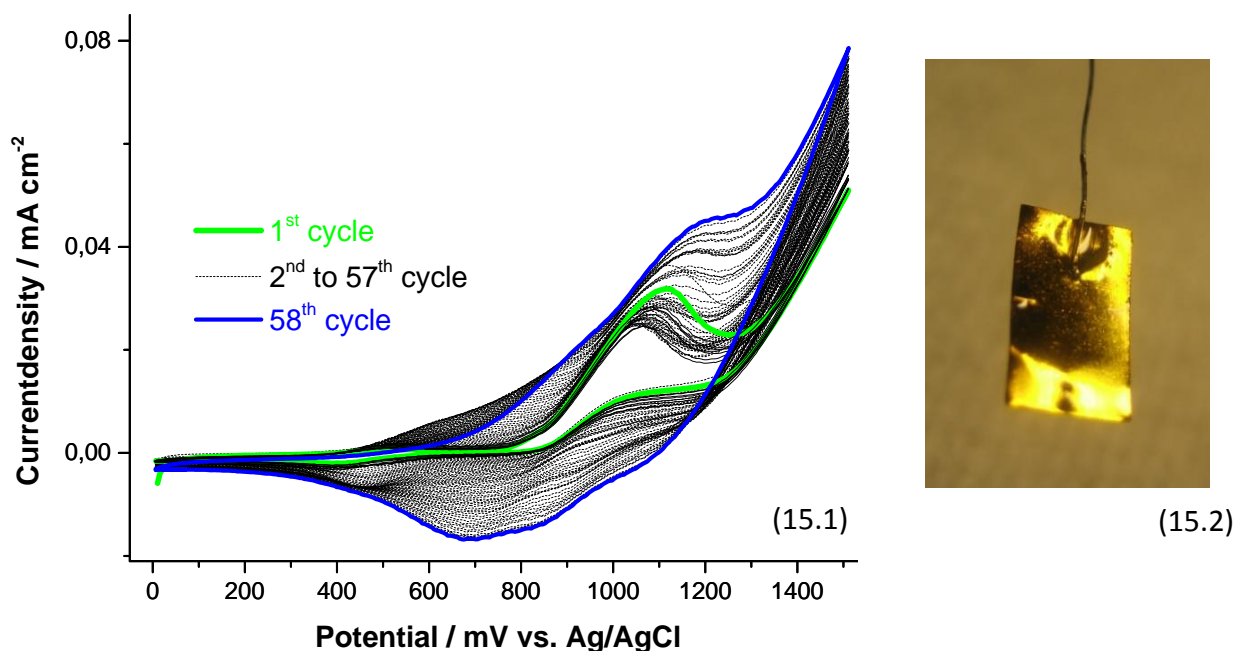


**Fig.15.** Cyclic voltammograms of the potentiodynamic electropolymerization of 23 mM  $fac-[Re(4\text{-methyl-4'-(7\text{-thienylheptyl})-2,2'\text{-bipyridine}(\text{CO})_3\text{Cl})]$  to  $P3[Re]HT$  (15.1) in BFEE/PPC (8 vol.%). First scan (green line) and last scan (blue line). The cyclic voltammograms were recorded at a scan rate of  $50\text{ mV s}^{-1}$  outside the glove box using a Pt working electrode (WE), a Pt counter electrode (CE) and a Ag/AgCl quasi reference electrode (RE). Picture of the “thick”  $P3[Re]HT$  film on the platinum sheet working electrode (15.2).

Fig.15 shows the potentiodynamic electropolymerization of 23 mM  $fac-[Re(4\text{-methyl-4'-(7\text{-thienylheptyl})-2,2'\text{-bipyridine}(\text{CO})_3\text{Cl})]$   $P3[Re]HT$  in a solution of boron trifluoride ethyl etherate containing propylene carbonate (8 vol.%). The successive film formation is indicated by an increase in the current density of each cycle. The first scan is depicted in green line and the last scan in blue line respectively. After electropolymerization the platinum working electrode was fully covered with a continuous, almost gold like shiny film.

Fig.16 shows the electroactivity of  $P3[Re]HT$ -“thick film” in propylene carbonate solution containing 0.1 M TBAPF<sub>6</sub> at various scan rates from  $100\text{ mV s}^{-1}$  (blue line) to  $10\text{ mV s}^{-1}$  (red line). As can be seen, similar to the reported behavior of poly(thiophene) and poly(3-hexylthiophene) before, the intensity of the redox wave currents is proportional to the scan rate and the polymer film exhibits reversible redox behavior. By comparing the electrochemical characterization of  $P3[Re]HT$ -“thin film” to  $P3[Re]HT$ -“thick film”, it is obvious that the conductivity of the film decreases roughly by a factor of about 10. This is most likely due to a strong steric interaction caused by the  $fac-[Re(2,2'\text{-bipyridyl})(\text{CO})_3\text{Cl}]$  groups attached to the poly(thiophene) backbone and hence the resistance of the material increases substantially with the thickness of the film.

### 3.3.4. Characterization of *P3[Re]HT*- "thick film"

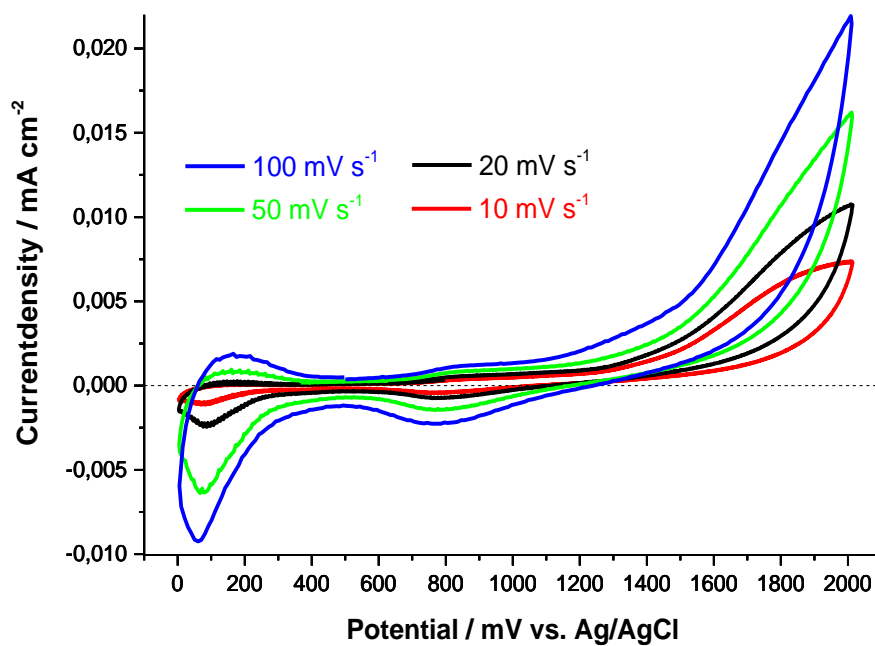


**Fig.16.** Cyclic voltammograms of a *P3[Re]HT*-“thick film” electrochemically polymerized on platinum plate electrode. The curves were recorded in propylene carbonate solution containing 0.1 M TBAPF<sub>6</sub> at different scan rates from 100 (blue line) to 10 (red line) mV s<sup>-1</sup>.

---

#### 4. Cyclic voltammetry studies on electrochemical CO<sub>2</sub> reduction

After the successful electrodeposition of poly(thiophene) and its derivatives on platinum sheet electrodes, the fully covered electrodes were transferred into an electrolyte solution containing no monomers and investigated towards electrochemical CO<sub>2</sub> reduction.

##### 4.1. Poly(thiophene)

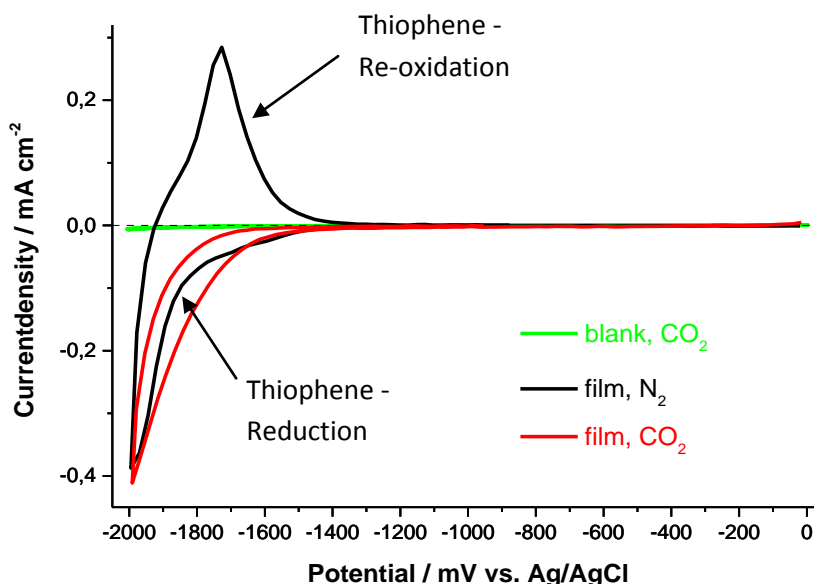


**Fig.17.** Cyclic voltammograms of poly(thiophene) electrodeposited on a platinum plate working electrode in ACN solution containing 0.1 M TBAPF<sub>6</sub> as supporting electrolyte. The electrolyte solution was purged for 15 minutes under stirring with nitrogen (black line) or CO<sub>2</sub> (green and red line) respectively before the measurement started. Cyclic voltammograms were recorded at 50 mV s<sup>-1</sup> inside the glove box using a Pt counter electrode (CE) and a Ag/AgCl quasi reference electrode (RE). The ferrocene peak half-wave potential  $E_{1/2 \text{Fc/Fc}^+}$  was measured at 415 mV vs. Ag/AgCl.

Fig.17 shows the electrochemical characterization of the electrodeposited poly(thiophene) on Pt sheet electrode from the experiment depicted in Fig.7.1 before. The characterization was carried out in ACN solution containing 0.1 M TBAPF<sub>6</sub> at a scan rate of 50 mV s<sup>-1</sup>. The electrolyte solution was purged with nitrogen (black line) or CO<sub>2</sub> (green and red line) for 15 minutes under stirring respectively before the measurement started. The reduction of poly(thiophene) starts at about -1600 mV vs. Ag/AgCl and is partly reversible with the re-oxidation maximum occurring at around -1700 mV vs. Ag/AgCl. If the carrier electrolyte solution was saturated with CO<sub>2</sub> this re-oxidation peak vanished.

## 4.2. Poly(3-hexylthiophene)

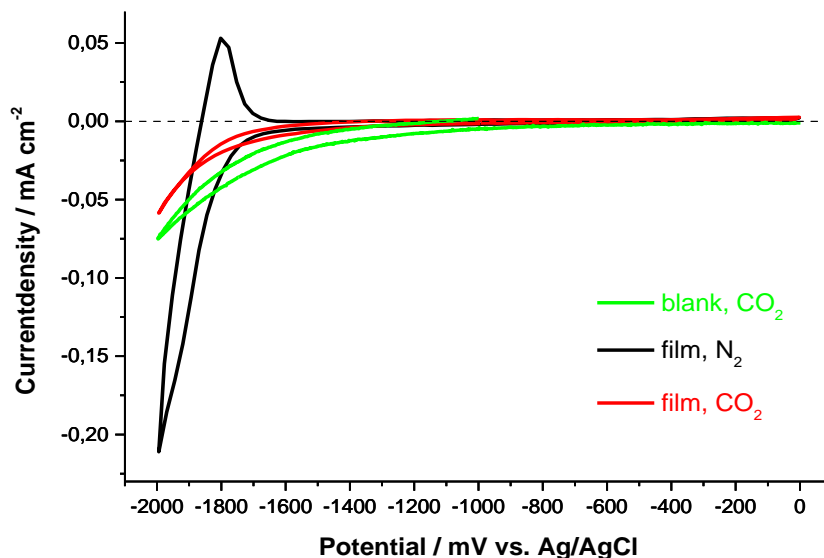


**Fig.18.** Cyclic voltammograms of poly(3-hexylthiophene) electrodeposited on a platinum plate working electrode in propylene carbonate solution containing 0.1 M TBAPF<sub>6</sub> as supporting electrolyte. The electrolyte solution was purged for 15 minutes under stirring with nitrogen (black line) or CO<sub>2</sub> (green and red line) respectively before the measurement started. Cyclic voltammograms were recorded at 50 mV s<sup>-1</sup> inside the glove box using a Pt counter electrode (CE) and a Ag/AgCl quasi reference electrode (RE). The ferrocene peak half-wave potential  $E_{1/2 \text{Fc}/\text{Fc}^+}$  was measured at 428 mV vs. Ag/AgCl.

Fig.18 shows the electrochemical characterization of the electrodeposited poly(3-hexylthiophene) on Pt sheet electrode from the experiment depicted in Fig.9.1 before. The characterization was carried out in propylene carbonate solution containing 0.1 M TBAPF<sub>6</sub> at a scan rate of 50 mV s<sup>-1</sup>. The electrolyte solution was purged with nitrogen (black line) or CO<sub>2</sub> (green and red line) for 15 minutes under stirring respectively, before the measurement started. The reduction of poly(3-hexylthiophene) starts at about -1700 mV vs. Ag/AgCl and is partly reversible with the re-oxidation maximum occurring at about -1850 mV vs. Ag/AgCl.

It is important to notice, that the magnitude of the reductive current is much lower if the carrier electrolyte solution was saturated with CO<sub>2</sub> compared to that of the curve obtained under inert (purged with nitrogen) electrolyte solution. Additionally, characteristic features of the poly(3-hexylthiophene) are not present any more. A similar behavior has been observed at our institute for a different class of organic semiconducting materials, namely Quinacridone (QNC). It was found that upon purging with CO<sub>2</sub> the characteristic reduction peak of QNC at -1480 mV diminished and the cathodic current decreased substantially showing similar features than represented in Fig.18.<sup>[38]</sup> This phenomenon was related to the formation of a QNC-carbonate salt and could be used for efficient and controlled CO<sub>2</sub> capture and release. In the case of QNC it was shown that 20 w% capture (20g CO<sub>2</sub>/ 100g QNC) could be achieved using controlled electrochemical reduce-and-capture. Since controlled capture, storage and release of CO<sub>2</sub> is a key step for both sequestration and

utilization of CO<sub>2</sub> these findings about organic semiconducting materials may become particularly interesting in the near future.

### 4.3. P3[Re]HT

#### 4.3.1. "Thin film" characterization

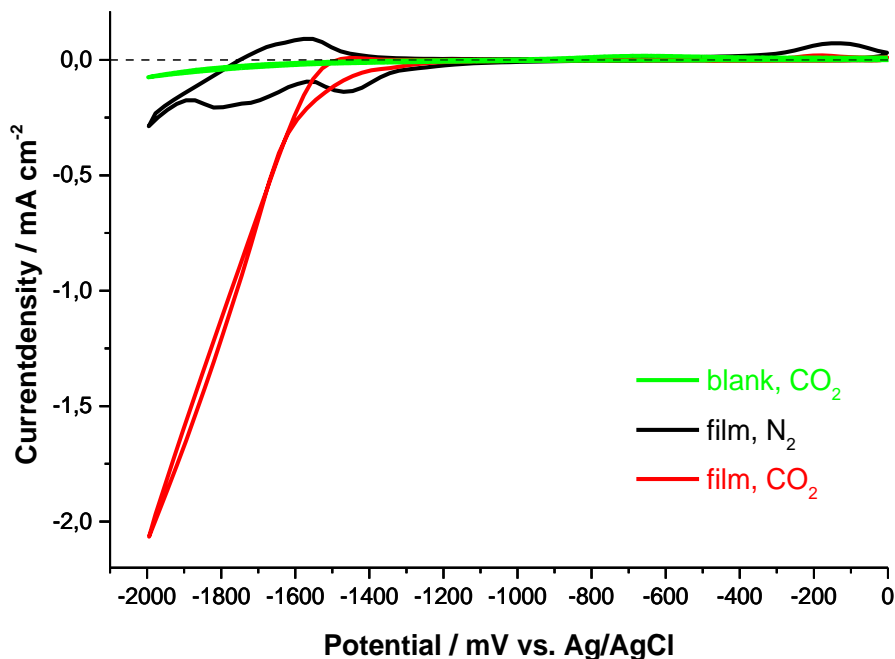


**Fig.19.** Cyclic voltammograms of *P3[Re]HT* electrodeposited on a platinum plate working electrode ("thin film") in propylene carbonate solution containing 0.1 M TBAPF<sub>6</sub> as supporting electrolyte. The electrolyte solution was purged for 15 minutes under stirring with nitrogen (black line) or CO<sub>2</sub> (green and red line) respectively before the measurement started. Cyclic voltammograms were recorded at 50 mV s<sup>-1</sup> inside the glove box using a Pt counter electrode (CE) and a Ag/AgCl quasi reference electrode (RE). The ferrocene peak half-wave potential  $E_{1/2\text{Fc}/\text{Fc}^+}$  was measured at 390 mV vs. Ag/AgCl.

Fig.19 shows cyclic voltammetric measurements of a *P3[Re]HT* "thin" film electrochemically deposited on Pt sheet electrode from the experiment depicted in Fig.11.1 before. The characterization was carried out in propylene carbonate solution containing 0.1 M TBAPF<sub>6</sub> at a scan rate of 50 mV s<sup>-1</sup>. The electrolyte solution was purged for 15 minutes under stirring with nitrogen (black line) or CO<sub>2</sub> (green and red line) respectively, before the measurement started. The measurement of an inert (purged with nitrogen) electrolyte solution did not show any reductive current in the potential window between 0 and -2000 mV vs. Ag/AgCl. If the electrolyte solution was purged with CO<sub>2</sub> and no polymerized catalyst - functionalized film was present, a minor reductive current started to flow at a potential lower than about -1800 mV vs. Ag/AgCl (green line). When the Pt working electrode covered with the "thin" film of *P3[Re]HT* was used for the measurement in the electrolyte solution under inert conditions, the typical reduction curve for a poly(thiophene) compound was measured showing low current densities upon a bias to -2000 mV vs. Ag/AgCl with current densities of

about  $-0.25 \text{ mA cm}^{-2}$ . If however the electrolyte solution is saturated with  $\text{CO}_2$ , a high, non-reversible reductive current enhancement is observed (red line).

The reductive current begins to increase at about  $-1550 \text{ mV}$  vs  $\text{Ag/AgCl}$  reaching current densities of about  $-2 \text{ mA cm}^{-2}$  at potentials of  $-2000 \text{ mV}$  vs.  $\text{Ag/AgCl}$ . This high reductive current density under  $\text{CO}_2$  saturation is even more promising, since the film characterization showed, that the conductivity of the polymer film is substantially lower than that of the bare Pt electrode.

Although a direct proof of reduction products is still missing, this current enhancement can be explained by a catalytic reduction of  $\text{CO}_2$  to  $\text{CO}$  by the *fac*-[ $\text{Re}(2,2'$ -bipyridyl)( $\text{CO}$ ) $_3\text{Cl}$ ] substituents attached to the poly(thiophene) backbone. Furthermore, the voltammogram under  $\text{CO}_2$  saturation shows peak crossing which is an inherent characteristic of the *fac*-[ $\text{Re}(2,2'$ -bipyridyl)( $\text{CO}$ ) $_3\text{Cl}$ ] catalyst during cyclic voltammetric measurements in  $\text{CO}_2$  saturated electrolyte solution.<sup>[39]</sup>

#### 4.3.2. "Thick film" characterization

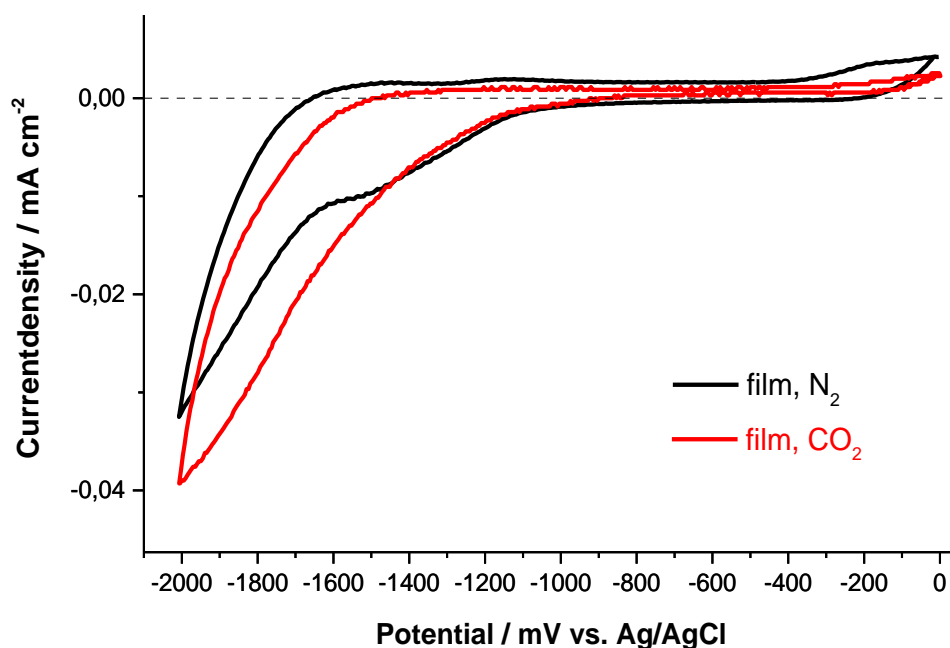


**Fig.20.** Cyclic voltammograms of *P3[Re]HT* electrodeposited on a platinum plate working electrode ("thick film") in propylene carbonate solution containing  $0.1 \text{ M TBAPF}_6$  as supporting electrolyte. The electrolyte solution was purged for 15 minutes under stirring with nitrogen (black line) or  $\text{CO}_2$  (red line) respectively, before the measurement started. Cyclic voltammograms were recorded at  $50 \text{ mV s}^{-1}$  inside the glove box using a Pt counter electrode (CE) and a  $\text{Ag/AgCl}$  quasi reference electrode (RE). The ferrocene peak half-wave potential  $E_{1/2 \text{Fc}/\text{Fc}^+}$  was measured at  $456 \text{ mV}$  vs.  $\text{Ag/AgCl}$ .

Fig.20 shows cyclic voltammetric measurements of a *P3[Re]HT* "thick" film electrochemically deposited on Pt sheet electrode from the experiment depicted in Fig.15.1 before. The characterization was carried out in propylene carbonate solution containing  $0.1 \text{ M TBAPF}_6$  at a scan rate of  $50 \text{ mV s}^{-1}$ . The electrolyte solution was purged for 15 minutes under stirring

with nitrogen (black line) or CO<sub>2</sub> (red line) respectively, before the measurement started. In the case of a CO<sub>2</sub> saturated electrolyte solution (red line) the magnitude of the reductive current was not significantly higher compared to that one in an inert electrolyte solution purged with nitrogen (black line).

The “thick” film of *P3[Re]HT* did not exhibit the same interesting electrochemical behavior between 0 and -2000 mV vs. Ag/AgCl compared to the “thin” film electrodeposited from the same monomer substance. Moreover, the order of magnitude of the reduction current was approximately 10 times lower in case of the “thick” film when compared to the one the “thin” film. That goes along with the observations obtained during characterization of both films for oxidative bias, as can be seen in Fig.14 and Fig.16.

## 5. Summary and Outlook

The monomer of the novel *fac*-[Re(2,2'-bipyridyl)(CO)<sub>3</sub>Cl] functionalized poly(3-hexylthiophene) was successfully synthesized several times. Two films of different thicknesses were electropolymerized from that material on platinum plates. Several additional attempts to reproduce the thin film functionalized polymer with the interesting electrochemical characteristics unfortunately failed. In presence of CO<sub>2</sub>, the "thin" film shows an interesting effect that is a strong indication of the activity of this new third-generation conductive polymer toward catalytic CO<sub>2</sub> reduction.

Compared to the complexed ligand *fac*-[Re(4,4'-dimethyl-2,2'-bipyridyl)(CO)<sub>3</sub>Cl] (Fig.9), the free ligand 4,4'-dimethyl-2,2'-bipyridene (Fig.10) did not show a partly irreversible oxidation wave starting at around 1300 mV vs. Ag/AgCl.

In order to prevent possible destruction of the *fac*-[Re(2,2'-bipyridyl)(CO)<sub>3</sub>Cl] group during electropolymerization a possibility would be to first electropolymerize the free ligand 4-methyl-4'-(7-(3-thienyl)-heptyl)-2,2'-bipyridine and, afterwards, complex the resulting polymer with Re(CO)<sub>5</sub>Cl to obtain *P3[Re]HT*.

Since Poly(3,4-ethylenedioxythiophene) (PEDOT) can be electropolymerized potentiodynamically by cycling between -900 and 1250 mV vs. Ag/AgCl<sup>[40]</sup>, it should be possible to electropolymerize a *fac*-[Re(2,2'-bipyridyl)(CO)<sub>3</sub>Cl] functionalized 3,4-ethylenedioxy-thiophene (EDOT) without running the risk of destroying the catalyst during electropolymerization.

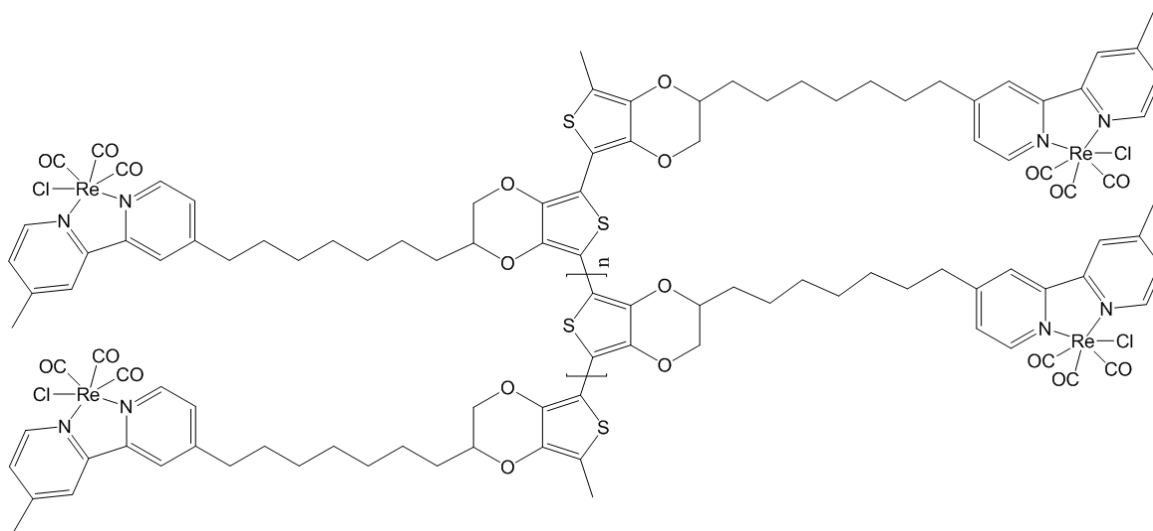


**Fig.21.** Schematic representation of *fac*-[Re(2,2'-bipyridyl)(CO)<sub>3</sub>Cl] - functionalized PEDOT.

Fig.21 shows the schematic representation of the *fac*-[Re(2,2'-bipyridyl)(CO)<sub>3</sub>Cl] - functionalized PEDOT. It is a hypothetical conjugated polymer with new physical and chemical properties for the potential applications of electro- and photochemical CO<sub>2</sub> reduction.

**References:**

- [1] Kerr, Richard, A. *Science* (80- ). **2007**, 317, 437.
- [2] Friedlingstein, P. *Nature* **2008**, 451, 297–298.
- [3] Yu, K. M. K.; Curcic, I.; Gabriel, J.; Tsang, S. C. E. *ChemSusChem* **2008**, 1, 893–899.
- [4] Balzani, V.; Credi, A.; Venturi, M. *ChemSusChem* **2008**, 1, 26–58.
- [5] Kumar, B.; Llorente, M.; Froehlich, J.; Dang, T.; Sathrum, A.; Kubiak, C. P. *Annu. Rev. Phys. Chem.* **2012**, 63, 541–569.
- [6] Spinner, N. S.; Vega, J. A.; Mustain, W. E. *Catal. Sci. Technol.* **2012**, 2, 19.
- [7] Benson, E. E.; Kubiak, C. P.; Sathrum, A. J.; Smieja, J. M. *Chem. Soc. Rev.* **2009**, 38, 89–99.
- [8] Spinner, N. S.; Vega, J. A.; Mustain, W. E. *Catal. Sci. Technol.* **2012**, 2, 19.
- [9] Kumar, B.; Llorente, M.; Froehlich, J.; Dang, T.; Sathrum, A.; Kubiak, C. P. *Annu. Rev. Phys. Chem.* **2012**, 63, 541–569.
- [10] Hawecker, J.; Lehn, J.; Ziessel, R. *J. Chem. Soc. Chem. Commun.* **1984**, 6, 328–330.
- [11] Hawecker, J.; Lehn, J.; Ziessel, R. *Helv. Chim. Acta* **1986**, 69, 1990–2012.
- [12] Sullivan, B. P.; Bolinger, C. M.; Conrad, D.; Vining, W. J.; Meyer, T. J. *J. Chem. Soc. Chem. Commun.* **1985**, 20, 1414–1416.
- [13] Yoshida, T.; Iida, T.; Shirasagi, T.; Lin, R.-J.; Kaneko, M. *J. Electroanal. Chem.* **1993**, 344, 355–362.
- [14] Cosnier, S.; Deronzier, A.; Moutet, J.-C. *J. Electroanal. Chem.* **1986**, 207, 315–321.
- [15] Yoshida, T.; Kamato, K.; Tsukamoto, M.; Iida, T.; Schlettwein, D.; Whrle, D.; Kaneko, M. *J. Electroanal. Chem.* **1995**, 385, 209–225.
- [16] Christensen, P.; Hamnett, A.; Muir, A. V. G.; Timney, J. A.; Higgins, S. *J. Chem. Soc. Faraday Trans.* **1994**, 90, 459.
- [17] Toole, T. R. O.; Sullivan, B. P.; Bruce, M. R.; Margerum, L. D.; Murray, R. W.; Meyer, T. *J. J. Electroanal. Chem.* **1989**, 259, 217–239.
- [18] Portenkirchner, E.; Gasiorowski, J.; Oppelt, K.; Schlager, S.; Schwarzinger, C.; Neugebauer, H.; Knör, G.; Sariciftci, N. S. *ChemCatChem* **2013**, 5, 1790–1796.

- [19] Sariciftci, N. S.; Mehring, M.; Gaudl, K. U.; Bäuerle, P.; Neugebauer, H.; Neckel, A. *J. Chem. Phys.* **1992**, *96*, 7164.
- [20] Heeger, A. J.; Sariciftci, N. S.; Nardas, E. B. *Semiconducting and Metallic Polymers*; Oxford University Press: New York, **2010**.
- [21] Garnier, F.; Tourillon, G.; Gizard, M.; Dubois, J. C. *J. Electroanal. Chem. Interfacial Electrochem.* **1983**, *148*, 299–303.
- [22] Mason, C. R.; Skabara, P. J.; Cupertino, D.; Schofield, J.; Meghdadi, F.; Ebner, B.; Sariciftci, N. S. *J. Mater. Chem.* **2005**, *15*, 1446.
- [23] Mozer, A.; Sariciftci, N.; Pivrikas, A.; Österbacka, R.; Juška, G.; Brassat, L.; Bässler, H. *Phys. Rev. B* **2005**, *71*, 035214.
- [24] Liao, S.; Li, Y.; Jen, T.; Cheng, Y.; Chen, S. *J. Am. Chem. Soc.* **2012**, *134*, 14271–14274
- [25] Wang, J.; Pappalardo, M.; Keene, F. *Aust. J. Chem.* **1995**, *48*, 1425.
- [26] Roncali, J. *Chem. Rev.* **1992**, *92*, 711-738.
- [27] *Advances in Electrochemical Science and Engineering*; Gerischer, H.; Tobias, C. W., Eds.; Wiley-VCH Verlag GmbH: Weinheim, Germany, **1991**, Vol. 2.
- [28] Sharma, P. S.; Pietrzyk-Le, A.; D'Souza, F.; Kutner, W. *Anal. Bioanal. Chem.* **2012**, *402*, 3177–3204.
- [29] Taylor, R. In *The Chemistry of Heterocyclic Compounds*; Gronowitz, S., Ed.; John Wiley and Sons: New York, 1986; Vol. 44, Part 2, pp. 1-118. (b) Kellogg, R. M. In *Comprehensive Heterocyclic Chemistry*; Katritzky, A. R., Rees, C. W., Eds.; Pergamon Press: Oxford, 1984; Vol. 4(3), p. 713. (c) Marino, G. *Adv. Heterocycl. Chem.* **1971**, *13*, 235.
- [30] Tanaka, K.; Shichiri, T.; Wang, S.; Yamabe, T. *Synth. Met.* **1988**, *24*, 203–215.
- [31] Xu, J.; Wei, Z.; Du, Y.; Pu, S.; Hou, J.; Zhou, W. *Journal of Applied Polymer Science* **2008**, *109*, 1570–1576.
- [32] Bard, A. J.; Faulkner, L. R. *Electrochemical Methods: Fundamentals and Applications*; 2 edition.; WILEY-VCH, 2000; p. 864.
- [33] Heinze, J. *Angew. Chemie* **1984**, *11*, 823 – 916.
- [34] Waltman, R. J.; Bargon, J.; Diaz, A. F. *J. Phys. Chem.* **1983**, *87*, 1459–1463.
- [35] Sato, M.; Tanaka, S.; Kaeriyama, K. *J. Chem. Soc. Chem. Commun.* **1985**, 713.
- [36] Wang, X.; Shi, G.; Liang, Y. *Electrochem. commun.* **1999**, *1*, 536–539.

- [37] Topchiev, A. V.; Zavgorodnii, S. V.; Paushkin, Y. M. *Boron Fluoride and Its Compounds As Catalysts in Organic Chemistry* **1959**, Pergammon Press: New York.
- [38] Apaydin, D. H.; Głowacki, E. D.; Portenkirchner, E.; Sariciftci, N. S. "Direct electrochemical capture and release of Carbon Dioxide using an industrial organic pigment: Quinacridone, *Angew. Chem. Int. Ed. Engl.*, **2014**, DOI: 10.1002/anie.201403618R1 (in press)
- [39] Portenkirchner, E.; Oppelt, K.; Ulbricht, C.; Egbe, D. a. M.; Neugebauer, H.; Knör, G.; Sariciftci, N. S. *J. Organomet. Chem.* **2012**, 716, 19–25.
- [40] Kvarnström, C.; Neugebauer, H.; Blomquist, S.; H.J. Ahonen, H. J.; Kankare, J.; Ivaska, A. *Electrochimica Acta* **1999**, 44, 2739–2750.

**Acknowledgements:**

I would like to thank all members of the Linz Institute for Organic Solar Cells (LIOS) for their friendliness and willingness to help.

In particular, great thanks to Dr. Elisa Tordin and Dr. Engelbert Portenkirchner for their support during my work and for equipping me with knowledge and skills necessary for further research into the field of electro- and photochemical CO<sub>2</sub> reduction .

My final thanks go to o.Univ. Prof. Mag. Dr. DDr. h.c. Niyazi Serdar Sariciftci for giving me the chance to do this very interesting work and providing me an insight into modern research in the field of physical chemistry.